Neural Network-Based Adaptive Control for Spacecraft Under Actuator Failures and Input Saturations

Zhou, Ning; Kawano, Yu; Cao, Ming

Published in:
IEEE Transactions on Neural Networks and Learning Systems

DOI:
10.1109/TNNLS.2019.2945920

Publication date:
2020

Neural Network Based Adaptive Control for Spacecraft under Actuator Failures and Input Saturations

Ning Zhou[1], *Member, IEEE*, Yu Kawano[2], *Member, IEEE*, Ming Cao[3], *Senior Member, IEEE*

***Abstract*—In this paper, we develop attitude tracking control methods for spacecraft as rigid bodies against model uncertainties, external disturbances, subsystem faults/failures, and limited resources. A new intelligent control algorithm is proposed using approximations based on radial basis function neural networks (RBFNN) and adopting the tunable parameter-based variable structure (TPVS) control techniques. By choosing different adaptation parameters elaborately, a series of control strategies are constructed to handle the challenging effects due to actuator faults/failures and input saturations. With the help of Lyapunov theory, we show that our proposed methods guarantee both finite-time convergence and fault-tolerance capability of the closed-loop systems. Finally, benefits of the proposed control methods are illustrated through five numerical examples.**

***Index Terms*—Attitude tracking, fault-tolerant control, input saturations, neural network control, finite-time control.**

I. Introduction

In the past decades, attitude control of spacecraft has attracted intensive research attentions in order to accomplish the various advanced space missions. Typically, attitude stabilization, attitude tracking, and attitude synchronization have been the central topics. More specifically for attitude tracking, its objective is to design an effective control law such that the motion of a spacecraft can track the desired attitude, which can be applied in, for example, the high-speed attitude reorientation of warning satellite in surveillance missions. The performance requirements, such as rapid response, high accuracy, and fault-tolerance, are essential to satisfy various attitude maneuvering commands under significant challenges caused by model uncertainties, external disturbances, subsystem failures, and limited resources (e.g., energy, memory space, and computing power) concurrently [1]. Moreover, in actual operation, the harsh operating conditions (e.g., coronal mass ejections from the Sun) may increase the possibility of malfunctions in spacecraft actuators and further lead to significant performance degradation or even task paralysis, and several failed aerospace missions occurred due to actuator faults and failures, e.g., the Kepler and FUSE space probes. Thus, research on fault-tolerance control of spacecraft also catches considerable attention of space engineers and scientists.

Promising results have been reported to address some of these problems, such as adaptive robust control [2], sliding mode control [3], [4], [5], intelligent control [3], [5], [6], [7], backstepping control [6], [8], hybrid control [9], active disturbance rejection control (ADRC) [10], event-triggered control [11], and optimal control [12]. However, it is still difficult to simultaneously handle finite-time convergence, model uncertainties, external disturbances, subsystem faults/failures, and input saturation at the same time, due to various strong nonlinearity in spacecraft dynamics., since spacecraft is a nonlinear system. For instance, there are some finite-time algorithms for spacecraft attitude control (e.g. [4], [12], [13], [14], [15], [16]), but [4], [12], [13], [14] and [15], [16] assume that actuators are fault-free and failure-free, respectively. In order to address undesirable actuator faults/failures, fault-tolerant control (FTC) strategies have been adopted, which can be classified into active FTC and passive FTC [17]. The former requires reconfigurations of a controller after a fault is found by a fault detection and diagnosis (FDD) scheme, while the latter tries to design a robust controller which addresses all expected faults a priori. Thus, the passive FTC is suitable for implementation in practice because it can avoid the time delay caused by online FDD and controller reconfiguration in contrast to active FTC. For such a reason, we follow a passive FTC approach.

In summary, our objective is to develop a passive FTC algorithm which guarantees finite-time convergence and fault-tolerance for attitude tracking under model uncertainties, external disturbances, and input saturations. The main idea is to employ two tools, namely radial basis function neural networks (RBFNN) approximations [18] and a tunable parameter-based variable structure (TPVS). The first one is to approximate unknown nonlinear functions of the spacecraft and is already employed to design tracking controllers in [19], [20], but we further develop computationally efficient methods. The latter technique is a novel extension of nonsingular fast terminal sliding mode (NFTSM) control [16] and is employed to achieve finite time convergence under actuator failures and input saturations, where these two realistic problem settings for actuators are not addressed by [16].

*This work of Zhou was supported in part by the National Natural Science Foundation of China under Grant 61603095 and Grant 61972093, by the Research Foundation for Outstanding Young Scholars in the University of Fujian Province, and by the Research Foundation for Outstanding Young Scholars in Fujian Agriculture and Forestry University under Grant XJQ201612. (Corresponding author: Ning Zhou.)

[1]Ning Zhou is with College of Computer and Information Sciences, Fujian Agriculture and Forestry University, 350002 Fuzhou, P. R. China. (zhouning2010@gmail.com).

[2]Yu Kawano is with the Graduate School of Engineering, Hiroshima University, Higashi-Hiroshima 739-8527, Japan. (ykawano@hiroshima-u.ac.jp).

[3]Ming Cao is with Faculty of Science and Engineering, University of Groningen, Nijenborgh 4, 9747 AG Groningen, the Netherlands. (m.cao@rug.nl).

More detailed explanations for differences from existing finite-time fault-tolerant controllers and intelligent fault-tolerant controllers are as follows.

Literature review: There are existing results on passive finite-time FTC and intelligent FTC. In comparison, the main contributions of our algorithm are clarified as follows. First, in order to deal with an unknown inertia matrix and the nonlinear characteristic of system, some finite-time FTC approaches are built upon linearization techniques, e.g. the linearized constraints associated with some scaled-up inequalities of system models (see [14], [15], [21], [22], [23], [24], [25]) and the linear regression (see [16], [26]). However, by applying these approaches, only local problems around an equilibrium point can be studied. Different from the linearization based approaches, to handle the unknown parameters and nonlinearity, the intelligent FTC methods have been proposed, e.g., the neural network FTC approach [6] and the fuzzy FTC approach [27]. However, these approaches lose the finite-time convergence property. In this paper, we further improve the neural network FTC method. In [6], the whole ideal weight matrix $W^* \in \mathbb{R}^{h\times m}$ ($h \times m$ parameters) of neural network is estimated, which requires intense computation. In order to solve this problem, we propose algorithms that only require an estimation of the supremum $\sup_{t\geq 0}\|W^*\|^2$, which significantly simplifies the design structure and reduces computational effort. Moreover, our approach guarantees finite-time convergence. Second, some of the existing finite-time FTC results and intelligent FTC results do not consider actuator saturation constraints although every actuator of a spacecraft has a saturation constraint in practice. For example, methods not considering actuator saturation constraints are the finite-time FTC approaches proposed in [14], [16], [23], [24], [25], [26] and the intelligent FTC method developed in [27]. In contrast, we also aim to design an algorithm that can handle actuator saturation constraints.

Contribution: The main contributions are emphasized as follows.

1) An RBFNN and TPVS based intelligent control algorithm is implemented to construct FTC strategies, which do not require prior information of the system parameters or faults/failures. In practice, both of them are difficult to identify beforehand.
2) A series of FTC strategies are presented for attitude tracking of spacecraft, which require less computation than conventional neural network control approach. Also, different from the existing intelligent FTC approaches, our method guarantees exponential or finite-time convergence of the tracking errors for nonlinear models.
3) An adaptive NN-based finite-time FTC scheme is proposed, and it accommodates undesirable actuator faults, subsystem failures, and limited resources, which has not been achieved for spacecraft attitude tracking by existing methods.

A preliminary conference version is found in [28] in which a controller taking into account actuation faults/failures, modelling uncertainties, and external disturbances is proposed. In this paper, we address, in addition, thrust limit for the actuator, and consequently develop control schemes further.

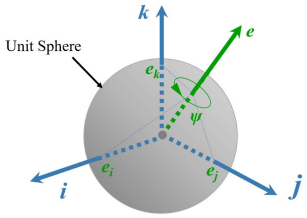

Fig. 1. A visualization of a rotation represented by unit quaternion, where $e = [e_i, e_j, e_k]^\top$ is the unit Euler axis, ψ is the Euler angle.

The rest of the paper is organized as follows: Section II presents preliminaries and control problem formulations; Section III elaborates the main results; Section IV provides examples to illustrated the proposed methods; finally, Section V concludes this paper.

Notation: The set of real numbers, positive real numbers, and non-negative real numbers are denoted by $\mathbb{R}$, $\mathbb{R}_{>0}$, and $\mathbb{R}_{\geq 0}$, respectively. For a vector or matrix, $\|\cdot\|$ denotes its Euclidean norm. The n-dimensional vector whose elements are all 1 is denoted by $\mathbb{1}_n \in \mathbb{R}^n$.

II. Preliminaries and Problem Formulation

A. Spacecraft Attitude Dynamics and Kinematics

The orientations and rotations of rigid spacecraft in 3-dimension can be represented by Euler angles, Cayley-Rodrigues parameters (CRPs), modified Rodrigues parameters (MRPs), or unit quaternion, etc. Compared with other mathods, the unit quaternion has no inherent geometrical singularity as do Euler angles, no singularities in the kinematical differential equations as do CRPs, and no requirement of solving the continuity of the description when switch occurs from the set to the shadow set at the singular point as do MRPs. As shown in Fig. 1, the unit quaternion defines the spacecraft attitude as an Euler-axis rotation in a unit sphere in the body reference frame $\mathcal{B}$ with respect to the inertial reference frame $\mathcal{I}$. The mathematical description of a unit quaternion is

$$q := \left[\cos(\psi/2)\,,\quad e^\top \sin(\psi/2)\right]^\top = [q_0, q_v^\top]^\top \in \mathbb{S}^3,$$

where $q_0 : \mathbb{R}_{\geq 0} \to \mathbb{R}^3$ and $q_v : \mathbb{R}_{\geq 0} \to \mathbb{R}^3$ are the scalar component and vector component of q, respectively, and $\mathbb{S}^3 := \{(q_0, q_v) \in \mathbb{R}\times\mathbb{R}^3 : q^\top q = q_0^2 + {q_v}^\top q_v = 1\}$. Taking the time derivative of each element of q, we get the kinematical differential equations as follows:

$$\begin{aligned}
2\dot{q}_0(t) &= -\omega_1(t)q_{v1}(t) - \omega_2(t)q_{v2}(t) - \omega_3(t)q_{v3}(t),\\
2\dot{q}_{v1}(t) &= \omega_1(t)q_0(t) - \omega_2(t)q_{v3}(t) + \omega_3(t)q_{v2}(t),\\
2\dot{q}_{v2}(t) &= \omega_1(t)q_{v3}(t) + \omega_2(t)q_0(t) - \omega_3(t)q_{v1}(t),\\
2\dot{q}_{v3}(t) &= -\omega_1(t)q_{v2}(t) + \omega_2(t)q_{v1}(t) + \omega_3(t)q_0(t),
\end{aligned}$$

where, $\omega : \mathbb{R}_{\geq 0} \to \mathbb{R}^3$ with $\omega := [\omega_1, \omega_2, \omega_3]^\top$ denotes the angular velocity with respect to the inertial frame $\mathcal{I}$ and expressed in the body frame $\mathcal{B}$. The above kinematical equations can be rewritten as follows:

$$\dot{q}_0(t) = -\frac{1}{2}q_v^\top(t)\omega(t). \tag{1}$$

$$\dot{q}_v(t) = \frac{1}{2}(q_v^\times(t) + q_0(t)I_3)\omega(t), \tag{2}$$

where the operators $q_v^\times : \mathbb{R}_{\geq 0} \to \mathbb{R}^{3\times 3}$ denote skew symmetric matrix acting on the vector q_v, which is given by

$$q_v^\times := \begin{bmatrix} 0 & -q_{v,3} & q_{v,2} \\ q_{v,3} & 0 & -q_{v,1} \\ -q_{v,2} & q_{v,1} & 0 \end{bmatrix}.$$

Consider a spacecraft equipped with $n > 3$ actuators rotating under the influence of body-fixed torquing devices. The Euler equation of motion about the principal axes of inertia is [29]:

$$J(t)\dot{\omega}(t) = -\omega^\times(t)J(t)\omega(t) + D\tau(t) + d(t), \tag{3}$$

where $\tau : \mathbb{R}_{\geq 0} \to \mathbb{R}^n$ denotes the control torque produced by n actuators. $d : \mathbb{R}_{\geq 0} \to \mathbb{R}^3$ represents the external disturbances. The matrix $J : \mathbb{R}_{\geq 0} \to \mathbb{R}^{3\times 3}$ denotes the inertia matrix-valued function expressed in $\mathcal{B}$, which is symmetric and positive definite, also see Remark 1 below, and $D \in \mathbb{R}^{3\times n}$ denotes the actuator distribution matrix. The operators $\omega^\times : \mathbb{R}_{\geq 0} \to \mathbb{R}^{3\times 3}$ denote skew symmetric matrices acting on the vector ω, which is given by

$$\omega^\times := \begin{bmatrix} 0 & -\omega_3 & \omega_2 \\ \omega_3 & 0 & -\omega_1 \\ -\omega_2 & \omega_1 & 0 \end{bmatrix}.$$

Remark 1. *According to [1], J depends on onboard payload, solar arrays, and fuel consumption and thus can change during an operation. Since it is difficult to identify $J(t)$ under each circumstance, this is assumed to be an unknown matrix-valued function; note that it is positive definite and bounded during the entire operation. In practice, it is reasonable to assume the boundedness of J, which is formally stated as Assumption 3 below.*

B. Modeling Actuator Faults/Failures and Input Saturation

The control torque τ is generated by actuators, which can be reaction wheels or thrusters. In general, actuators have maximum allowable torques and may be burned out in the middle of a mission. Therefore, a model of control torque needs to consider saturations, faults and failures. According to the definitions of faults and failures in [21] and [30], respectively, the control torque of each actuator is modeled as follows:

$$\tau_i(t) = e_i(t)u_{c,i}(t) + \bar{u}_i(t),\ i = 1,\dots,n,\ n > 3, \tag{4}$$

and its compact form is

$$\tau(t) = E(t)u_c(t) + \bar{u}(t), \tag{5}$$

where $u_c : \mathbb{R}_{\geq 0} \to \mathbb{R}^n$ and $\bar{u} : \mathbb{R}_{\geq 0} \to \mathbb{R}^n$ denote the desired torque signal of the ith actuator generated by the controller and the uncertain faulty input entering the spacecraft in an additive way, respectively; $e_i : \mathbb{R}_{\geq 0} \to [0, 1]$ denotes the effectiveness factor of the ith actuator, and $E := \mathrm{diag}\{e_1, e_2, \dots, e_n\}$.

According to [21], [30], there are four main possibilities of faults/failures, which are summarized in Table I. Note that in the fault-free case, $e_i = 1$ and $\bar{u}_i = 0$, and thus $\tau_i = u_{c,i}$, $i = 1, 2, \dots, n$.

In general, the input saturation can be described as follows: $|u_{c,i}(\cdot)| \leq u_{\max}$, $i = 1,\dots,n$, with the constant $u_{\max} > 0$ being the maximum allowable input of the ith actuator control torque.

TABLE I
RELATIONS BETWEEN MODEL PARAMETERS AND ACTUATOR FAULTS OR FAILURES

Fault or Failure	Type	e_i	$\bar{u}_i$
Fault 1	Partial loss of effectiveness fault	$0 < e_i < 1$	$\bar{u}_i = 0$
Fault 2	Bias fault	$e_i = 1$	$\bar{u}_i \neq 0$
Failure 1	Outage failure	$e_i = 0$	$\bar{u}_i = 0$
Failure 2	Hardover failure	$e_i = 0$	$\bar{u}_i \neq 0$

C. Attitude Tracking Error System

Our goal in this paper is to solve an attitude tracking problem to a reference denoted by $(w^d, q_0^d, q_v^d) : \mathbb{R}_{\geq 0} \to \mathbb{R}^3 \times \mathbb{S}^3$, where $(q_0^d(\cdot))^2 + q_v^d(\cdot)^\top q_v^d(\cdot) = 1$ with respect to the internal frame $\mathcal{I}$ and expressed in the desired frame $\mathcal{D}$. Now, we define the attitude tracking error $(\tilde{q}_0, \tilde{q}_v) : \mathbb{R}_{\geq 0} \to \mathbb{S}^3$ as the relative orientation between the body frame $\mathcal{B}$ and the desired frame $\mathcal{D}$, which satisfies $\tilde{q}_0^2(\cdot) + \tilde{q}_v(\cdot)^\top \tilde{q}_v(\cdot) = 1$ and can be calculated by the quaternion multiplication rule in [31] as follows:

$$\tilde{q}_v = q_0^d q_v - q_0 q_v^d + q_v^\times q_v^d, \tag{6}$$

$$\tilde{q}_0 = q_0^d q_0 + (q_v^d)^\top q_v. \tag{7}$$

Assume that the desired angular velocity ω^d is bounded as $\|\omega^d(\cdot)\| \leq \bar{\omega}_1$ and $\|\dot{\omega}^d(\cdot)\| \leq \bar{\omega}_2$ by some unknown constants $\bar{\omega}_1 \geq 0$ and $\bar{\omega}_2 \geq 0$. The corresponding rotation matrix-valued function is a proper orthogonal matrix given by $R = \left(\tilde{q}_0^2 - \tilde{q}_v^\top \tilde{q}_v\right) I_3 + 2\tilde{q}_v\tilde{q}_v^\top - 2\tilde{q}_0\tilde{q}_v^\times$, and it satisfies $\|R(\cdot)\| = 1$ and $\dot{R} = -\tilde{\omega}^\times R$. The angular velocity error $\tilde{\omega} : \mathbb{R}_{\geq 0} \to \mathbb{R}^3$ in $\mathcal{B}$ with respect to $\mathcal{D}$ is represented as

$$\tilde{\omega} = \omega - R\omega^d. \tag{8}$$

From (3) – (8), the attitude tracking error dynamics and kinematics can be derived as follows [29]:

$$J(t)\dot{\tilde{\omega}} = -\omega^\times J(t)\omega + J(t)\left(\tilde{\omega}^\times R(t)\omega^d - R(t)\dot{\omega}^d\right) + DE(t)u_c + DE(t)\bar{u} + d, \tag{9}$$

$$\dot{\tilde{q}}_v = \frac{1}{2}\left(\tilde{q}_v^\times + \tilde{q}_0 I\right)\tilde{\omega}, \tag{10}$$

$$\dot{\tilde{q}}_0 = -\frac{1}{2}\tilde{q}_v^\top \tilde{\omega}. \tag{11}$$

In this paper, we impose the following practically reasonable assumptions for controller design.

Assumption 1. *[32] There exists an unknown nonnegative constant $d_{\max}$ such that the external disturbance d is bounded by $\|d(\cdot)\| \leq d_{\max}$.*

Assumption 2. *There exists an unknown nonnegative constant $\bar{u}_{\max}$ such that the additive fault $\bar{u}$ in (5) is bounded by $\|\bar{u}(\cdot)\| \leq \bar{u}_{\max}$.*

Assumption 3. *There exists positive constants $J_{\min}$, $J_{\max}$ and J_d such that $J_{\min} \leq \|J(\cdot)\| \leq J_{\max}$ and $0 \leq \|\frac{dJ(\cdot)}{dt}\| \leq J_d$.*

Assumption 4. *[21] The number of totally failed actuators is no more than $n-3$, i.e., the matrix $DED^\top$ is positive definite, and there exists a positive constant $e_{\min}$ such that*

$$e_{\min} \leq \lambda_{\min}(DE(\cdot)D^\top), \tag{12}$$

where $\lambda_{\min}(\cdot)$ denotes the minimum eigenvalue of a matrix.

Remark 2. *If Assumption 4 does not hold, then the matrix $DED^\top$ becomes singular, and the system is under-actuated, which is beyond the scope of our interest in this paper. Furthermore, we only assume the existence of $e_{\min}$, and its value is not needed for controller design.*

D. Tunable Parameter-Based Variable Structures

In this paper, we design a sliding mode controller to stabilize the tracking error in finite time under model uncertainties. The main idea is to capture both error dynamics of $\tilde{\omega}$ and $\tilde{q}_v$ by a single variable S, and this idea is from the approach of using a tunable parameter-based variable structure (TPVS). This is possible because the dimensions of $\tilde{\omega}$ and $\tilde{q}_v$ are the same.

To introduce a TPVS, we need to define several functions by using $\tilde{\omega}$ and $\tilde{q}_v$. First, two functions $\bar{\sigma}_1 : \mathbb{R}^3 \times \mathbb{R}^3 \to \mathbb{R}^3$ and $\bar{\sigma}_2 : \mathbb{R}^3 \times \mathbb{R}^3 \to \mathbb{R}^3$ are defined as

$$\begin{aligned}
&\bar{\sigma}_{1,i}(\tilde{\omega}_i, \tilde{q}_{v,i}) := \tilde{\omega}_i + c_1\tilde{q}_{v,i} + c_2\tilde{q}_{v,i}^{[r]},\\
&\bar{\sigma}_{2,i}(\tilde{\omega}_i, \tilde{q}_{v,i}) := \tilde{\omega}_i + c_1\tilde{q}_{v,i} + c_2(l_1\tilde{q}_{v,i} + l_2\tilde{q}_{v,i}^{[2]}),\\
&\quad l_1 := (2-r){\phi_q}^{r-1},\ l_2 := (r-1){\phi_q}^{r-2},\\
&\quad \tilde{q}_{v,i}^{[s]} := |\tilde{q}_{v,i}|^s \mathrm{sgn}(\tilde{q}_{v,i}),\ s > 0,\ i = 1,2,3,
\end{aligned}$$

where $c_1, c_2, \phi_q > 0$, $r \in (1/2, 1)$ and $\mathrm{sgn}(\cdot)$ is the sign function that returns -1, 0 or 1. Next, by using these $\bar{\sigma}_{1,i}$ and $\bar{\sigma}_{2,i}$, define a switching function $\sigma : \mathbb{R}^3 \times \mathbb{R}^3 \to \mathbb{R}^3$ as

$$\begin{aligned}
&\sigma_i(\bar{\sigma}_{1,i}, \bar{\sigma}_{2,i})\\
&:= \begin{cases} \bar{\sigma}_{2,i}(\tilde{\omega}_i, \tilde{q}_{v,i}) & \text{if } \bar{\sigma}_{1,i}(\tilde{\omega}_i, \tilde{q}_{v,i}) \neq 0,\ |\tilde{q}_{v,i}| \le \phi_q,\\ \bar{\sigma}_{1,i}(\tilde{\omega}_i, \tilde{q}_{v,i}) & \text{otherwise,} \end{cases}\\
&i = 1,2,3.
\end{aligned} \tag{13}$$

Now, we are ready to introduce a TPVS $S : \mathbb{R}^3 \to \mathbb{R}^3$ as a function of σ:

$$S_i(\sigma_i) := \varrho\left(\sigma_i - \bar{\epsilon}\mathrm{sat}(\sigma_i)\right),\ i = 1,2,3, \tag{14}$$

$$\mathrm{sat}\left(\sigma_i\right) := \begin{cases} \mathrm{sgn}(\sigma_i), & \text{if } |\sigma_i/\bar{\epsilon}| \ge 1,\\ \sigma_i/\bar{\epsilon}, & \text{if } |\sigma_i/\bar{\epsilon}| < 1, \end{cases} \tag{15}$$

where $\varrho > 0$ and $\bar{\epsilon} \in (0,1)$. Note that the constants $c_1, c_2, \phi_q, \varrho > 0$, $r \in (1/2, 1)$ and $\bar{\epsilon} \in (0,1)$ are design parameters.

One notices that $S_i(\sigma_i) = 0$ if and only if $|\sigma_i/\varepsilon_i| \le 1$. Therefore, if one designs a control law such that $S_i(\sigma_i) = 0$, then $|\sigma_i| \le \bar{\epsilon}$ is guaranteed, which implies that the tracking errors $\tilde{\omega}_i$ and $\tilde{q}_{i,v}$ are bounded from the definition of σ_i. Moreover, according to the following lemma, the boundedness of S implies those of $\tilde{\omega}$ and $\tilde{q}_v$. These facts suggest to design a controller which stabilizes S.

Lemma 1. *Consider the TPVS $S(t)$ defined by (14). For any $\bar{\delta}_1 > 0$, $\tilde{q}_v(0) \in \mathbb{R}^3$ with $\|\tilde{q}_v(0)\| \le 1$, if $\|S(\cdot)\| \le \bar{\delta}_1$, then there exists a settling time $T_*(\tilde{q}_v(0), \bar{\delta}_1) > 0$ such that*

$$|\tilde{q}_{v,i}(t)| \le \max\{\bar{\delta}_2, \phi_q\}, \tag{16}$$

$$|\tilde{\omega}_i(t)| \le \bar{\delta}_1/\varrho + \bar{\epsilon} + c_1\max\{\bar{\delta}_2, \phi_q\} + c_2(\max\{\bar{\delta}_2, \phi_q\})^r, \tag{17}$$

$$\bar{\delta}_2 := \min\left\{\frac{\bar{\delta}_1/\varrho}{c_1 - \bar{c}_1}, \left(\frac{\bar{\delta}_1/\varrho}{c_2 - \bar{c}_2}\right)^{1/r}\right\} \tag{18}$$

for all $i = 1,2,3$ and $t \ge T_*(\tilde{q}_v(0), \bar{\delta}_1)$, where $\bar{c}_1$ and $\bar{c}_2 > 0$ are selected to satisfy $c_1 > \bar{c}_1$ and $c_2 > \bar{c}_2$.

The proof is given in Appendix A. In Lemma 1, for smaller $\bar{c}_1$ and $\bar{c}_2 > 0$, δ_2 is smaller. However, as shown in its proof in Appendix A, for smaller $\bar{c}_1$ and $\bar{c}_2 > 0$, the convergence of $|\tilde{q}_{v,i}(t)|$ and $|\tilde{\omega}_i(t)|$ are slower, but are still within finite time.

Now, we compute the dynamics of S. Since $\tilde{\omega}$ and $\tilde{q}_v$ are functions of the time, $S(\sigma(\tilde{\omega}(t), \tilde{q}_v(t)))$ is also a function of the time. By abusing notation, we use $S(t)$ to describe $S(\sigma(\tilde{\omega}(t), \tilde{q}_v(t)))$. By taking its time derivative, we have

$$\frac{1}{\varrho}J(t)\dot{S} = F(t,z) + D(t)E(t)u_c + D(t)\bar{u} + d - \frac{1}{2\varrho}\dot{J}(t)S, \tag{19}$$

$$\begin{aligned}
F(t,z) &:= -\omega^\times J(t)\omega + J(t)(\tilde{\omega}^\times R(t)\omega^d - R(t)\dot{\omega}^d) + \frac{1}{2\varrho}\dot{J}(t)S\\
&\quad + \frac{1}{2}J(t)c_1(\tilde{q}_v^\times + \tilde{q}_0 I_3)\tilde{\omega} + J(t)c_2\dot{\alpha},
\end{aligned} \tag{20}$$

$$z := \begin{bmatrix} \omega^\top & (\omega^d)^\top & (\dot{\omega}^d)^\top & q_v^\top & \alpha^\top & \dot{\alpha}^\top \end{bmatrix}^\top \tag{21}$$

for the region of $(\tilde{w}, \tilde{q}_v)$ such that $|\sigma_i/\bar{\epsilon}| > 1$, $i = 1,2,3$, where $\alpha : \mathbb{R}^3 \times \mathbb{R}^3 \to \mathbb{R}^3$ is the following switching function:

$$\begin{aligned}
&\alpha_i(\tilde{q}_{v,i}, \bar{\sigma}_{1,i})\\
&:= \begin{cases} l_1\tilde{q}_{v,i} + l_2\tilde{q}_{v,i}^{[2]} & \text{if } \bar{\sigma}_{1,i}(\tilde{\omega}_i, \tilde{q}_{v,i}) \neq 0,\ |\tilde{q}_{v,i}| \le \phi_q,\\ \tilde{q}_{v,i}^{[r]} & \text{otherwise,} \end{cases}\\
&i = 1,2,3,
\end{aligned}$$

and this can be viewed as a function of the time like S. Note that $\sigma = \tilde{\omega} + c_1\tilde{q}_v + c_2\alpha$ and $\alpha = [\alpha_1, \alpha_2, \alpha_3]^\top$.

Remark 3. *The TPVS is a generalization of a nonsingular fast terminal sliding mode (NFTSM) proposed by [16]. The difference between the TPVS and the NFTSM is that the TPVS has the parameter ϱ and the boundary layer term $\bar{\epsilon}\mathrm{sat}(\sigma_i)$, which can increase the degrees of freedom for robust controller design. When $\varrho = 1$ and $\bar{\epsilon} = 0$, i.e. $S(\sigma) = \sigma$, the TPVS reduces to the NFTSM. In function σ_i, the coefficients l_1 and l_2 are selected to make $d\sigma_i/dt$, $i = 1,2,3$ as a continuous function of the time, see [33].*

E. Neural Networks Based Function Approximation

In this paper, we use the dynamics of TPVS (19) for controller design. However, as mentioned in Remark 1, J is an unknown function of the time, and so F in (20) is unknown. The existence of these unknown parameters, especially F makes control design challenging, since F also depends on other functions such as w and q_v nonlinearly. To overcome this design difficulty arising from the nonlinearity and uncertainty, the universal approximation property of radial basis function neural networks (RBFNN) [18] is adopted for controller design.

First, we review the universal approximation property of RBFNN. Consider to represent a continuous nonlinear function $\bar{F} : \mathbb{R}^l \to \mathbb{R}^m$ (that does not depend on t) by using a matrix $\bar{W}^* \in \mathbb{R}^{h \times m}$ and a basis function vector $\bar{\varphi} : \mathbb{R}^l \to \mathbb{R}^h$, where h is called the number of neurons, $\bar{\varphi}_k(z) := \exp[-(z - \bar{\mu}_k)^\top(z - \bar{\mu}_k)/(2\bar{\psi}_k^2)]$ for $k = 1,2,\ldots,h$, $\bar{\mu}_k \in \mathbb{R}^l$ denotes the center of the receptive field, $\bar{\psi}_k \in \mathbb{R}$ denotes the width of the Gaussian function, and $0 < \bar{\varphi}_k(z) \le 1$. According to the

universal approximation property of RBFNN, for any $\bar{\varepsilon}_N > 0$, there exist a prefixed compact set $\Omega_z \subset \mathbb{R}^l$ that can be made as large as desired, a positive integer h, a matrix $\bar{W}^*$, and a basis function vector $\bar{\varphi}$ such that

$$\bar{F}(z) = (\bar{W}^*)^\top \bar{\varphi}(z) + \bar{\varepsilon}(z), \ \forall z \in \Omega_z, \tag{22}$$

where $\|\bar{\varepsilon}(\cdot)\| \leq \bar{\varepsilon}_N$.

Now, by selecting $l = 18$, $m = 3$, we consider to approximate the function F in (20). Even though it depends on t, by using the time-dependent matrix $W^* : \mathbb{R}_{\geq 0} \to \mathbb{R}^{h\times 3}$, for any $\varepsilon_N > 0$, there exist a prefixed sufficiently large compact set $\Omega_z \subset \mathbb{R}^{18}$, a positive integer h, a time-varying matrix $W^*(t) \in \mathbb{R}^{h\times 3}$, and a basis function vector $\varphi : \mathbb{R}^{18} \to \mathbb{R}^h$ such that F can be described as:

$$F(t,z) = (W^*(t))^\top \varphi(z) + \varepsilon_0(t,z), \ \forall t \in \mathbb{R}_{\geq 0}, z \in \Omega_z, \tag{23}$$

where $\|\varepsilon_0(\cdot,\cdot)\| \leq \varepsilon_N$. By substituting (23) into (19), we have

$$\begin{aligned}\frac{1}{\varrho} J(t)\dot{S} =& (W^*(t))^\top \varphi(z) + \varepsilon_0(t,z) \\ &+ D(t)E(t)u_c + D(t)\bar{u} + d - \frac{1}{2\varrho}\dot{J}(t)S.\end{aligned} \tag{24}$$

In this paper, we design a controller based on equation (24). In particular, the dynamics of u_c is designed to achieve the aforementioned control objectives. We further suppose that $|\sigma_i/\bar{\epsilon}| > 1$, $i = 1,2,3$, and z is in a prefixed sufficiently large compact set $\Omega_z \subset \mathbb{R}^{18}$ for all $t \in \mathbb{R}_{\geq 0}$. For the designed controllers, we restrict our interest to solutions to the closed-loop systems that satisfy the above two properties for σ_i and z. We use symbol S^* with the asterisk $*$ to denote S corresponding to such solutions. Throughout the paper, the asterisk $*$ stands for similar meanings for any variables.

Remark 4. *In the conventional methods [19], [20], all the elements of matrix W^* are estimated for controller design. However, we only estimate $\sup_{t\geq 0}\|W^*(t)\|$, where this is bounded from Assumption 3. Since we only estimate this upper bound that is a constant instead of a matrix-valued function of t, our methods simplify the controller design and reduce computational burden.*

F. Control Objectives

The overall control objective of this paper is to design effective fault-tolerant attitude tracking control algorithms, such that the following requirements are achieved progressively under actuation faults/failures, input saturation, modeling uncertainties, and external disturbances.

1) For any positive constant $\bar{\delta}_1 > 0$ and for any initial value $(S^*(0), \hat{\theta}_1^*(0)) \in \mathbb{R}^3 \times \mathbb{R}$, the error $\|S^*(t)\|$ converges to a value less than $\bar{\delta}_1$ exponentially as $t \to +\infty$, where $\hat{\theta}_1^*(0)$ is the initial value of the adaptive design parameter $\hat{\theta}_1 : \mathbb{R}_{\geq 0} \to \mathbb{R}$ specified in (26). Note that as mentioned before, if $\|S_i(t)\| = 0$, then $|\sigma_i| \leq \bar{\epsilon}$ is guaranteed for given $\bar{\epsilon} \in (0,1)$, which implies that the tracking errors $|\tilde{\omega}_i|$ and $|\tilde{q}_{i,v}|$ are within the allowed level.
2) For any positive constant $\bar{\delta}_1 > 0$ and for any initial value $(S^*(0), \hat{\theta}^*(0), \hat{\eta}^*(0)) \in \mathbb{R}^3 \times \mathbb{R} \times \mathbb{R}$, there exists a finite $T_*(\tilde{q}_v(0), \bar{\delta}_1) > 0$ such that (16) and (17) hold for any $t \geq T_*(\tilde{q}_v(0), \bar{\delta}_1) > 0$, where $\hat{\theta}, \hat{\eta} : \mathbb{R}_{\geq 0} \to \mathbb{R}$ are the adaptive design parameters specified in (28) and (29). Therefore, the tracking errors $|\tilde{\omega}_i|$ and $|\tilde{q}_{i,v}|$ are within the allowed level in finite time.
3) The control objective 2) is achieved under the input saturations $|u_{c,i}(\cdot)| \leq u_{\max}$, $i = 1,\ldots,n$, with $u_{\max} > 0$.

III. Controller Design

We first take into account the situation in which there are actuation faults/failures, modelling uncertainties, and external disturbances, but there is no thrust limit for the actuators. Then, we provide three controllers which achieve objectives 1), 2), and 3) in Section II-F, respectively. In our conference version [28], the controller in Section III-A is proposed, but the controllers in Sections III-B and III-C are new. Especially, the controller in Section III-C addresses the actuation limit.

A. NN-based Controller for Exponential Convergence

To achieve the control objective 1) in Section II-F, we employ the following dynamic controller:

$$u_c = -\left(K_S + \hat{\theta}_1 \frac{\|\Phi(z)\|}{\|S\|}\right) D^\top S, \tag{25}$$

$$\dot{\hat{\theta}}_1 = \gamma_S \|S\| \|\Phi(z)\| - \gamma_\theta \hat{\theta}_1, \tag{26}$$

where $\hat{\theta} : \mathbb{R}_{\geq 0} \to \mathbb{R}$, $\Phi(\cdot) := [\varphi^\top(\cdot), 1]^\top$, and the positive constants K_S, γ_S, and γ_θ are design parameters.

For the closed-loop system, we have the following convergence result of the TPVS S. The proof is given in Appendix B.

Theorem 1. *Suppose that Assumptions 1–4 hold. Then, one can design the parameters of a TPVS and controller dynamics (25) and (26) such that the following holds: for any positive constant $\bar{\delta}_1 > 0$ and for any $(S^*(0), \hat{\theta}_1^*(0)) \in \mathbb{R}^3 \times \mathbb{R}$, the Euclidean norm of the solution to the closed loop system consisting of (24)–(26), $\|S^*(t)\|$ converges to $\bar{\delta}_1$ exponentially.*

The approach proposed in Theorem 1 only guarantees the convergence of S, which does not guarantee the convergence of the tracking errors $\tilde{\omega}$ and $\tilde{q}_v$. To pursue faster response and higher control accuracy, we focus on developing finite-time methods in the following sections, i.e., achieving the control objective 2) in Section II-F.

B. Adaptive NN-Based Finite-time Control under Actuator Failure

To achieve the control objective 2), we employ the following adaptive NN-based controller:

$$u_c = -\left(K_\phi \|S\|^2 + K_S + \frac{(K_\rho + \hat{\eta})}{\|S\|} + \frac{\|\varphi(z)\|^2}{\phi_\theta}\hat{\theta}\right) D^\top S, \tag{27}$$

$$\dot{\hat{\theta}} = \frac{1}{\phi_\theta}\gamma_S \|\varphi(z)\|^2 \|S\|^2 - \gamma_\theta \hat{\theta}, \tag{28}$$

$$\dot{\hat{\eta}} = \frac{1}{\alpha}\|S\| - \gamma_\eta \hat{\eta}. \tag{29}$$

where $\hat{\theta}, \hat{\eta} : \mathbb{R}_{\geq 0} \to \mathbb{R}$, and positive constants K_ϕ, K_S, K_ρ, ϕ_θ, γ_S, γ_θ, α and γ_δ are design parameters.

Then, we have the following convergence result. The proof is given in Appendix C

Theorem 2. *Suppose that Assumptions 1–4 hold. Then, one can design a TPVS and controller dynamics (27)–(29) such that the following holds: for any positive constant $\bar{\delta}_1 > 0$, there exists a finite $T_*(\tilde{q}_v(0), \bar{\delta}_1) > 0$ such that (16) and (17) hold for any $t \geq T_*(\tilde{q}_v(0), \bar{\delta}_1) > 0$.*

C. Adaptive NN-Based Finite-Time Control under Actuator Failure and Input Saturation

Finally, we also address the actuation limit on each actuator, i.e. the control requirement 3). As the actuator limit, we consider the case $|u_{c,i}(\cdot)| \leq u_{\max}$, $i = 1, \ldots, n$, with $u_{\max} > 0$ mentioned in Section II-B. Therefore, we design control inputs with saturations:

$$u_c := \hbar(\bar{u}_c)\bar{u}_c, \tag{30}$$

where $\bar{u}_c : \mathbb{R}_{\geq 0} \to \mathbb{R}^n$ is needed to be further designed. The function $\hbar$ is introduced to represent the saturation, where $\hbar := \mathrm{diag}\{\hbar_1, \ldots, \hbar_n\}$, and $\hbar_i : \mathbb{R} \to (0, 1]$, $i = 1, \ldots, n$ is defined as

$$\hbar_i(\bar{u}_{c,i}) := \begin{cases} \frac{u_{\max}}{\bar{u}_{c,i}} \mathrm{sign}(\bar{u}_{c,i}) & \text{if } |\bar{u}_{c,i}| > u_{\max}, \\ 1 & \text{if } |\bar{u}_{c,i}| \leq u_{\max}. \end{cases} \tag{31}$$

From (30), the saturation of $\bar{u}_c$, namely u_c are the actual control inputs. To achieve the control objective 3), we design $\bar{u}_c$ as follows:

$$\begin{aligned} \bar{u}_c =& - D^\top \left(K_\phi \|S\|^2 + K_S + \frac{1}{\phi_\theta} \hat{\theta} \|\varphi(z)\|^2 \right) S \\ & - D^\top \xi \hat{\zeta} \frac{(K_\rho + \hat{\eta})S}{\|S\|}, \end{aligned} \tag{32}$$

$$\dot{\hat{\theta}} = \frac{1}{\phi_\theta} \gamma_S \|S\|^2 \|\varphi(z)\|^2 - \gamma_\theta \hat{\theta}, \tag{33}$$

$$\dot{\hat{\eta}} = \alpha^{-1} \|S\| - \gamma_\eta \hat{\eta}, \tag{34}$$

$$\dot{\hat{\zeta}} := \begin{cases} 0 & \text{if } \hat{\zeta} = 1 \text{ and } \zeta_\hbar < 0, \\ \zeta_\hbar & \text{otherwise}, \end{cases} \tag{35}$$

$$\zeta_\hbar := \beta \xi \hat{\zeta}^3 ((K_\varrho + \hat{\eta}) \|S\| - \gamma_\zeta \hat{\zeta}), \ \hat{\zeta}(0) > 1$$

where $\hat{\theta}, \hat{\eta} : \mathbb{R}_{>0} \to \mathbb{R}$, $\hat{\zeta} : \mathbb{R}_{>0} \to \mathbb{R}_{>0}$ and positive constants K_ϕ, K_S, ϕ_θ, K_ρ, $\xi > 1$, γ_S, γ_θ, α, γ_η, β and γ_ζ are design parameters.

Hereafter, we impose a reasonable assumption, which states that the system remains full-actuated as discussed in Remark 2.

Assumption 5. *The number of totally failed actuators is no more than $n-3$, i.e., the matrix $DE\hbar D^\top$ is positive definite, and there exists a positive constant $\bar{e}_{\min}$ such that*

$$\bar{e}_{min} \leq \lambda_{\min}(DE(\cdot)\hbar(\cdot)D^\top), \tag{36}$$

where the ith element of $\hbar : \mathbb{R} \to (0, 1]^{n \times n}$ is defined in (31).

From Assumption 5 and Lemma 5 in Appendix D, there exists $M > 0$ such that $-M \leq \bar{u}_{c,i}(\cdot) \leq M$, $i = 1, \ldots, n$. Furthermore, there exists $0 < \underline{\zeta} \leq 1$ such that

$$\underline{\zeta} \leq \hbar_i(\bar{u}_{c,i}), \ \forall \bar{u}_{c,i} \in [-M, M], \ \forall i = 1, \ldots, n. \tag{37}$$

In (35), we introduce a new adaptation parameter $\hat{\zeta}$. This can be viewed as an estimation of $1/\underline{\zeta} \geq 1$, which is designed to compensate the energy fading of $\bar{u}_c$ caused by actuator faults and failures. Note that the adaptation law (35) guarantees that $\hat{\zeta} \geq 1$ for $\hat{\zeta}(0) \geq 1$, which corresponds to $1/\underline{\zeta} \geq 1$. Note that the term $-\gamma_\zeta \hat{\zeta}$ in $\zeta_\hbar$ is used to prevent the increase of adaptive gain $\hat{\zeta}$.

Now, we are ready to propose the following result. The proof is given in Appendix D.

Theorem 3. *Suppose that Assumptions 1–3 and 5 hold. Then, one can design a TPVS and controller dynamics (30)–(35) such that the following holds: 1) for any positive constant $u_{\max}$, the designed control input satisfies $|u_{c,i}(\cdot)| \leq u_{\max}$, $i = 1, \ldots, n$; 2) for any positive constant $\bar{\delta}_1 > 0$, there exists a finite $T_*(\tilde{q}_v(0), \bar{\delta}_1) > 0$ such that (16) and (17) hold for any $t \geq T_*(\tilde{q}_v(0), \bar{\delta}_1) > 0$.*

In Theorem 3, we have designed a controller which guarantees finite-time convergence and fault-tolerance for attitude tracking under model uncertainties, external disturbances, and input saturations. The proposed controller has the following futures in comparison with the related existing controllers.

1) Different from the linearized based FTC approaches, our methods can handle the unknown parameters and nonlinearity. Moreover, finite-time convergence is guaranteed in contrast to existing nonlinear methods.
2) In addition, less computational effort is required than the neural network based FTC, which does not guarantee finite-time convergence. The reason is that our method only tunes the estimation of the supremum of the ideal weight matrix $W^* \in \mathbb{R}^{h \times m}$ rather than the whole matrix W^*.
3) Compared with most of the existing finite-time FTC and intelligent FTC results, the proposed algorithm handles actuator saturation, which makes it more practical and competitive than the related existing results.

Therefore, the proposed controller can handle more realistic scenarios than existing ones.

Remark 5. *Control laws (27) and (32) are discontinuous due to the functions $D^\top \frac{(K_\rho + \hat{\eta})S}{\|S\|}$ and $D^\top \xi \hat{\zeta} \frac{(K_\rho + \hat{\eta})S}{\|S\|}$, which may lead to undesirable control chattering. As discussed in [34], this problem can be alleviated by replacing the discontinuous terms with the continuous terms $D^\top \frac{(K_\rho + \hat{\eta})S}{\|S\| + \varepsilon_c}$ and $D^\top \xi \hat{\zeta} \frac{(K_\rho + \hat{\eta})S}{\|S\| + \varepsilon_c}$, respectively, where ε_c is a sufficiently small positive constant.*

Remark 6. *In our proposed algorithm, there are two phases in the dynamics of the closed-loop systems, namely the reaching and sliding phases. The reaching phase corresponds to the dynamics before getting close to the sliding surface. The sliding phase corresponds to the dynamics on the sliding surface. The convergence speed and precision of the tracking errors in the reaching phase can be adjusted by tuning K_S, K_ρ, ξ and ϱ. When the other three parameters are fixed, the greater K_S (K_ρ, ξ, ϱ) is, the faster the convergence speed and the better the convergence precision are. In the sliding phase, the convergence speed and precision of the tracking*

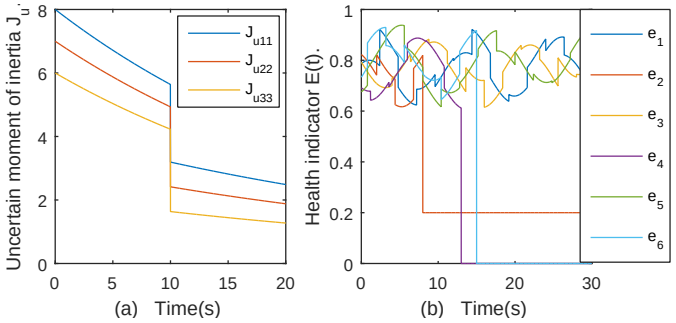

Fig. 2. (a) Uncertain moment of inertia J_u; (b) Health indicator $E(t)$.

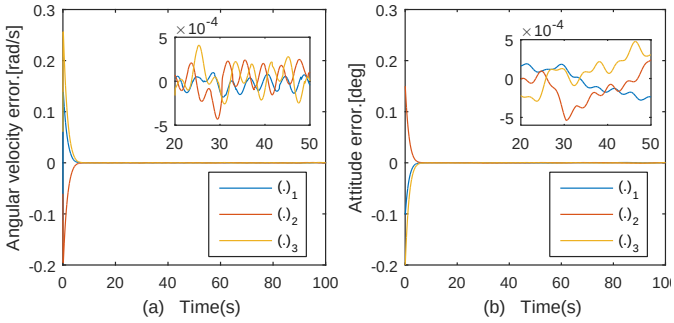

Fig. 3. Time response of tracking errors using controller u_c in Eq. (27). (a) $\tilde{\omega}$; (b) $\tilde{q}_v$.

errors can be adjusted by tuning c_1, c_2 and r. The greater c_1 and c_2 are, the faster the convergence speed and the better the convergence precision are; the smaller r is, the faster the convergence speed and the better the convergence precision are. Therefore, by tuning these parameters, one can adjust the convergence speed and precision of the tracking errors as fast and accurately as desired.

IV. Simulations

To evaluate the performance of the proposed algorithms in *Theorems 2* and *3*, simulations on a vehicle with six thrusters are conducted.

First, we give the simulation data of the system model. The unknown and time varying inertia matrix is $J(t) = J_0 + J_u(t)$, where J_0 is given by

$$J_0 = \begin{bmatrix} 20 & 0 & 0.9 \\ 0 & 17 & 0 \\ 0.9 & 0 & 15 \end{bmatrix} \text{kg} \cdot \text{m}^2,$$

and $J_u(t)$ is shown in Fig. 2 (a). The thruster distribution matrix D and the disturbance torque d are selected as in [1],

$$D = \begin{bmatrix} 0.8 & -0.8 & 0 & 0 & 0 & 0 \\ 0 & 0 & 0.7 & -0.7 & 0 & 0 \\ 0 & 0 & 0 & 0 & 0.7 & -0.7 \end{bmatrix}.$$

The health indicator $E(t)$ is depicted in Fig. 2 (b). The additive bias torque $\bar{u}$ is chosen as in [16] and the maximum available torque is considered to be $u_{\max} = 2\text{Nm}$. The time-varying desired angular velocity is given by

$$\omega^d(t) = [0.1\cos(0.1t), -0.1\sin(0.1t), 0.1\cos(0.1t)]^\top \text{rad/s}.$$

Second, the initial attitude $q_v(0)$ is selected as in [1]. The initial angular velocity is $\omega(0) = [0, 0, 0]^\top$. The initial value of the tracking errors $\tilde{q}_v(0)$ and $\tilde{\omega}(0)$ can be calculated according to (6) and (8).

Third, we use 6 neurons for each NN, and the sigmoid basis functions are applied with the center of the receptive field $\mu_k = k - 3$ and the width of the Gaussian function $\psi_k = \sqrt{2}$ for $k = 1, 2, \ldots, 6$.

Five examples are simulated in this section, which are 1) thrusters with actuator faults/failures, 2) healthy thrusters with limited thrusts, 3) thrusters with limited thrusts and actuator faults/failures, 4) influence of design parameters on control performance, and 5) comparison with other algorithms for spacecraft attitude stabilization.

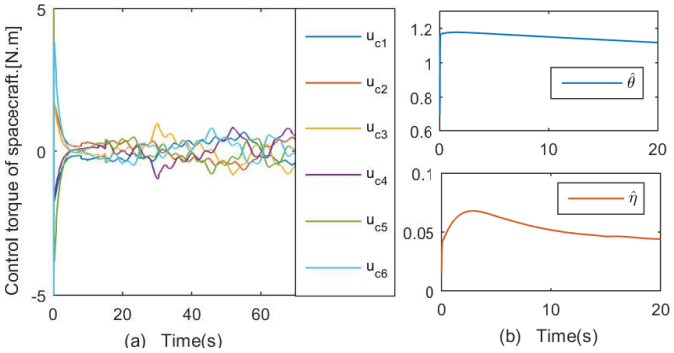

Fig. 4. (a) Time response of controller u_c in (27); (b) Design parameters in (28) and (29).

A. Thrusters with Actuator Faults/Failures

This subsection represents a severe case of the thrusters to demonstrate the effectiveness and performance of the control scheme designed in *Theorems 2*.

We select the design parameters $\varrho = 40$, $\bar{\epsilon} = 10^{-4}$, $c_1 = 1$, $c_2 = 0.2$, $\phi_q = 0.01$ and $r = 0.66$, which are used to calculate S in (14). Then we choose the design parameters $K_\phi = 0.01$, $K_S = 20$, $\phi_\theta = 0.1$, $K_\rho = 0.01$, $\varepsilon_c = 0.007$, which are used to compute u_c in (27). Next, we give the initial value of the adaptive parameters $\hat{\theta}(0) = 0.1$, $\hat{\eta}(0) = 0.001$ and select the design parameters $\gamma_S = 0.1$, $\gamma_\theta = 0.003$, $\alpha = 10$, $\gamma_\eta = 0.06$, which are used to calculate $\hat{\theta}$ and $\hat{\eta}$ according to (28)–(29).

As illustrated in Fig. 2(b), the health level of each thruster is generated by the same function given as in [1]. The angular velocity and attitude tracking errors are presented in Fig. 3. It is obvious that the controller (27) can provide not only high precision attitude tracking performance ($|\tilde{\omega}_i| \leq 5 \times 10^{-4}\text{deg/s}$, $|\tilde{q}_{vi}| \leq 5.4 \times 10^{-4}\text{deg}$, $i = 1, 2, 3$, during the period of 20s∼50s) but also fault tolerance capability. Fig. 4(a) shows the driving torque of the spacecraft with the control action beyond its maximum allowable limit 2Nm. The adaptive parameters $\hat{\theta}$ and $\hat{\eta}$ are shown in Fig. 4(b). It is observed that $\hat{\theta}$ and $\hat{\eta}$ are bounded, thus the efficacy of the proposed adaptation laws in (26)-(28) is verified.

B. Healthy Thrusters with Limited Thrusts

Applying the control scheme designed in *Theorem 3*, we aim to demonstrate the effectiveness and performance of the

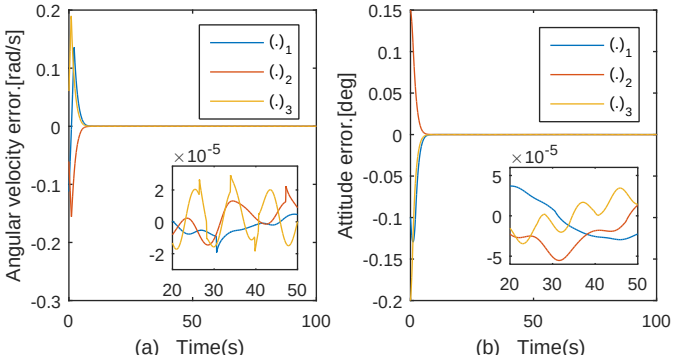

Fig. 5. (a) Time response of tracking errors using controller u_c in Eq. (30). (a) $\tilde{\omega}$; (b) $\tilde{q}_v$.

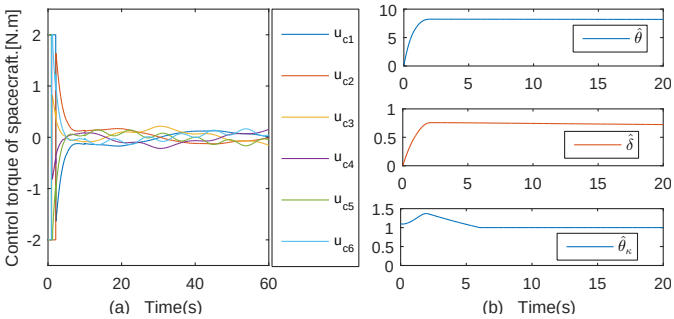

Fig. 6. (a) Time response of controller u_c in (30); (b) Time response of adaptive parameters $\hat{\theta}$, $\hat{\eta}$, and $\hat{\zeta}$ in (33) and (34).

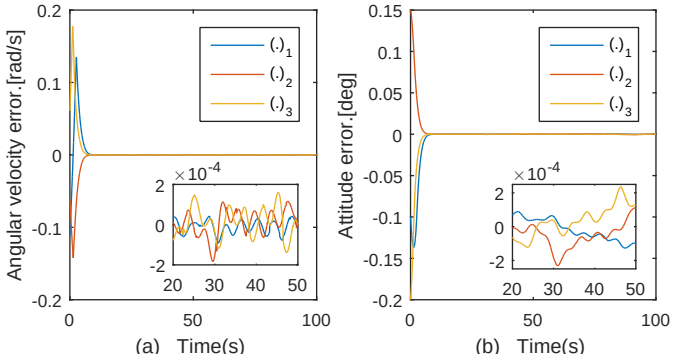

Fig. 7. Time response of tracking errors using controller u_c in Eq. (30). (a) $\tilde{\omega}$; (b) $\tilde{q}_v$.

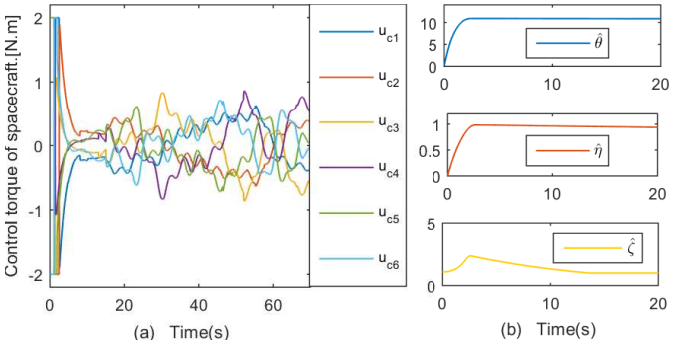

Fig. 8. (a) Time response of controller u_c in (30); (b) Time response of adaptive parameters $\hat{\theta}$, $\hat{\eta}$, and $\hat{\zeta}$ in (33) and (34).

method with all thrusters functioning healthily. The involved controller parameters, adaptation parameters and initial values are given as Section IV-A. As shown in Fig. 5, the angular velocity and attitude tracking errors converge to $|\tilde{\omega}_i| \leq 3 \times 10^{-5}$deg/s and $|\tilde{q}_{vi}| \leq 5.6 \times 10^{-5}$deg during the period of 20s∼50s respectively for $i = 1, 2, 3$. One can observe higher control precision and better tracking process in Fig. 5 than in Fig. 3. This indicates that the influence of actuator faults/failures is more significant on control precision than the influence of actuator input saturation. The control torques u_c produced by six thrusters and the adaptive parameters $\hat{\theta}$, $\hat{\eta}$, and $\hat{\zeta}$ are depicted in Fig. 6. One can observe that the control torques in Fig. 6(a) and the adaptive parameters $\hat{\theta}$, $\hat{\eta}$, and $\hat{\zeta}$ in Fig. 6(b) are all bounded, which verified the efficacy of the proposed control scheme in *Theorems 3*.

C. Thrusters with Limited Thrusts and Actuator Faults/Failures

In this subsection, we aim to examine the effectiveness and performance of the control scheme designed in *Theorem 3* while considering the actuator failure and input saturation simultaneously.

We select the design parameters $\varrho = 40$, $\bar{\epsilon} = 10^{-4}$, $c_1 = 1$, $c_2 = 0.2$, $\phi_q = 0.01$, and $r = 0.66$, which are used to calculate S in (14). Then we choose the design parameters $K_\phi = 0.01$, $K_S = 40$, $\phi_\theta = 0.1$, $\xi = 1.1$, $K_\rho = 0.01$, and $\varepsilon_c = 0.007$, which are used to compute $\bar{u}_c$ in (32). Next, we give the initial value of the adaptive parameters $\hat{\theta}(0) = 0.1$, $\hat{\eta}(0) = 0.001$, $\hat{\zeta}(0) = 1.1$, and select the design parameters $\gamma_S = 0.1$, $\gamma_\theta = 0.003$, $\alpha = 10$, $\gamma_\eta = 0.06$, $\beta = 0.08$, $\gamma_\zeta = 0.08$, which are used to calculate $\hat{\theta}$, $\hat{\eta}$, and $\hat{\zeta}$ according to (33)–(35).

Fig. 7 shows the angular velocity and attitude tracking errors which can converge to $|\tilde{\omega}_i| \leq 1.8 \times 10^{-4}$deg/s and $|\tilde{q}_{vi}| \leq 2.3 \times 10^{-4}$deg during the period of 20s∼50s respectively for $i = 1, 2, 3$. The convergence precision of $\tilde{\omega}_i$ and $\tilde{q}_{vi}$ in this subsection is worse than that in Subsection IV-C due to the adverse effect from actuator faults/failures. Fig. 8 shows the control torques u_c produced by six thrusters (Fig. 8(a)) and the adaptive parameters $\hat{\theta}$, $\hat{\eta}$, and $\hat{\zeta}$ (Fig. 8(b)), which are all bounded. Thus the efficacy of the proposed method in *Theorems 3* is verified.

D. Influence of Design Parameters on Control Performance

To investigate effects of several key design parameters, we use the following three control performance indices.

$$\text{CPI}_1 = \|\tilde{q}_v\|, \ \text{CPI}_2 = \|\tilde{\omega}\|, \ \text{CPI}_3 = \|u_c\|.$$

From the simulation data in Tables II and III, we observe that, when the other parameters are fixed, the greater ϱ (c_1, c_2, K_S, ξ, K_ρ) is, the higher control precision we get. Furthermore, the smaller $\bar{\epsilon}$ (K_ϕ) is, the better control precision we obtain. These results are consistent with our analysis in Remark 6.

E. Comparison with Other Algorithms for Spacecraft Attitude Stabilization

In this subsection, we adopt the three indices to study the control performance of the proposed algorithm comparing with

TABLE II
RESPONSE OF THE THREE INDICES AT 200S USING DIFFERENCE PARAMETERS IN (14)

ϱ	$\bar{\epsilon}$	c_1	c_2	CPI_1	CPI_2	CPI_3
10	10^{-4}	1	0.2	3.768×10^{-4}	5.32×10^{-4}	0.4985
20	10^{-4}	1	0.2	1.048×10^{-4}	1.26×10^{-4}	0.494
20	10^{-2}	1	0.2	1.466×10^{-4}	1.356×10^{-4}	0.5274
20	10^{-4}	0.1	0.2	4.547×10^{-4}	4.4622×10^{-4}	0.5108
20	10^{-4}	1	0.1	1.803×10^{-4}	1.889×10^{-4}	0.4933

TABLE III
RESPONSE OF THE THREE INDICES AT 200S USING DIFFERENCE PARAMETERS IN (32)

K_ϕ	K_S	ξ	K_ρ	CPI_1	CPI_2	CPI_3
0.01	20	1.1	0.01	1.048×10^{-4}	1.26×10^{-4}	0.494
0.1	20	1.1	0.01	1.077×10^{-4}	1.307×10^{-4}	0.4923
0.01	40	1.1	0.01	7.928×10^{-5}	9.481×10^{-5}	0.4756
0.01	20	1.7	0.01	7.687×10^{-5}	9.434×10^{-5}	0.4794
0.01	20	1.1	0.1	1.006×10^{-4}	1.244×10^{-4}	0.4831

the two finite-time FTC algorithms given in [21] and [22], which are built upon linearization technique for spacecraft attitude stabilization. Since the algorithms in [21] and [22] can only be applied to the problem of spacecraft attitude stabilization, we choose $q_v^d = [0,0,0]^\top$ and $\omega^d = [0,0,0]^\top$ in the proposed algorithm. Using the system model data in this paper, all the design parameters in this comparison are selected the same as the original data in the corresponding algorithms except the sliding mode control gains $\alpha = 1$ and $\beta = 0.2$ in [21]. Using the same computer and selecting the same sampling period, the running time and the response of the indices of the three algorithms are shown in Table IV and Figs. 9–11, respectively. By observing and comparing the simulation results, it concludes that the proposed approach provides faster convergence and better control precision of the indices than the algorithms in [21] and [22].

TABLE IV
RUNNING TIME OF THREE ALGORITHMS

Controller	(32)	(42) in [21]	(17) in [22]
Runing time	5.0637×10^{-3}s	5.075×10^{-3}s	5.0877×10^{-3}s

V. CONCLUSION

This paper studied finite-time attitude tracking control problems for rigid spacecraft under model uncertainty, fault-tolerance, and thrust limits. A series of control strategies were proposed by implementing the RBFNN and TPVS based intelligent control algorithms. The proposed control schemes were independent of any accurate model information. The control performances are analyzed based on Lyapunov stability theory. Numerical simulations on three severe actuation cases have shown the effectiveness of the proposed approaches.

In this paper, we developed a state-dependent approach. To seek methods requiring only sensor output information, one can design observers as Laplace ℓ_1 Huber based Kalman filter [35] and sliding mode observers [36], [37]. Currently, we are working on developing observer based algorithms.

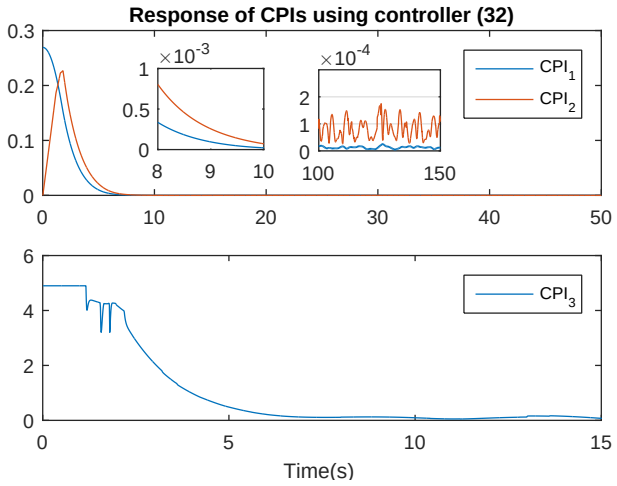

Fig. 9. Time response of the three indices using controller u_c in (32).

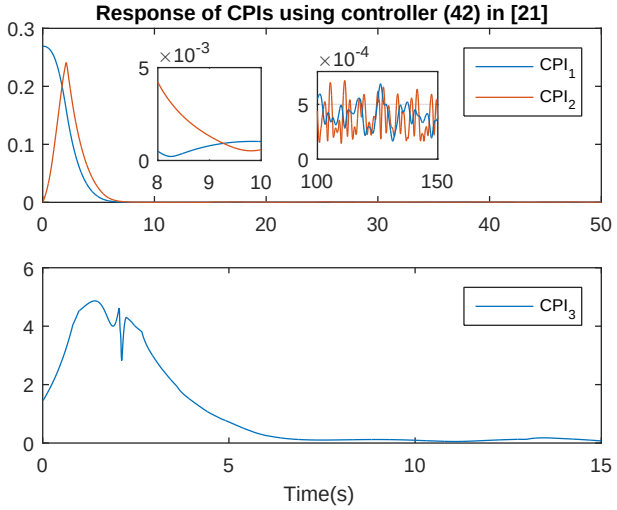

Fig. 10. Time response of the three indices using controller (42) in [21].

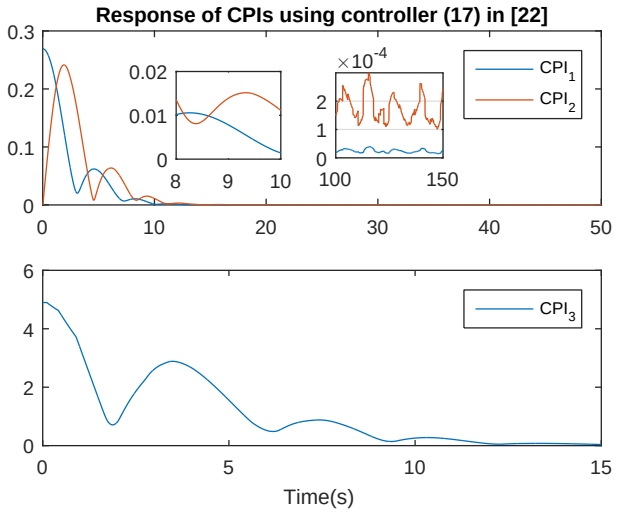

Fig. 11. Time response of the three indices using controller (17) in [22].

APPENDIX A
LEMMAS

Some instrumental lemmas are introduced here.

Lemma 2. *For any $e \in \mathbb{R}_{>0}$ and $\theta, \hat{\theta} \in \mathbb{R}$, the following inequality holds.*

$$(\theta - e\hat{\theta})\hat{\theta} \leq -\tfrac{1}{2e}(\theta - e\hat{\theta})^2 + \tfrac{1}{2e}\theta^2.$$

Proof: Define $\tilde{\theta} := \theta - e\hat{\theta}$. Then, compute

$$\begin{aligned}(\theta - e\hat{\theta})\hat{\theta} &= \tilde{\theta}(\theta - \tilde{\theta})/e \\ &= -\tilde{\theta}^2/e + \tilde{\theta}\theta/e \leq -\tilde{\theta}^2/e + |\tilde{\theta}||\theta|/e.\end{aligned}$$

From Young's inequality, $|\tilde{\theta}||\theta| \leq \tilde{\theta}^2/2 + \theta^2/2$.
Therefore, we have $(\theta - e\hat{\theta})\hat{\theta} \leq -\tilde{\theta}^2/(2e) + \theta^2/(2e)$.
By substituting $\tilde{\theta} = \theta - e\hat{\theta}$ into the above inequality, we obtain the statement of the lemma. ∎

Lemma 3. *[38] Let $x = 0$ be an equilibrium point of system $\dot{x} = f(x)$, i.e., $f(0) = 0$, where $x \in \mathbb{R}^3$, and $f : \mathbb{R}^3 \to \mathbb{R}^3$ is continuous. Let $\Omega_x \subset \mathbb{R}^3$ be a domain containing $x = 0$ in its interior. Let $V : \mathbb{R}_{\geq 0} \times \Omega_x \to \mathbb{R}$ be a continuously differentiable function such that*

$$W_1(x) \leq V(t,x) \leq W_2(x), \tag{38}$$

$$\frac{\partial V}{\partial t} + \frac{\partial V}{\partial x}\frac{\partial x}{\partial t} \leq -\mu_1 V - \mu_2 V^{\nu} \tag{39}$$

for all $t \geq 0$ and $x \in \Omega_x$, where $W_1(x)$ and $W_2(x)$ are continuous positive definite functions on Ω_x, $\mu_0, \mu_1, \mu_2 > 0$, and $\nu \in (0,1)$. Then $x = 0$ is finite-time stable. The settling time can be calculated by

$$T_{\text{reach}} \leq [1/(\mu_1(1-\nu))]\ln(\mu_1 V_0^{1-\nu}/\mu_2 + 1) \quad \text{for (39)},$$

where $V_0 := V(t_0, x(t_0))$ and t_0 is the initial time.

Finally, we prove Lemma 1 in Section II.

Proof of Lemma 1: For any $\bar{\delta}_1 > 0$, if $\|S(\cdot)\| \leq \bar{\delta}_1$, then $|S_i(\cdot)| \leq \bar{\delta}_1$, $|\sigma_i| \leq \bar{\delta}_0$ hold with $\bar{\delta}_0 := \bar{\delta}_1/\varrho + \bar{\epsilon}$. Three cases are considered based on the definition of $\sigma_i(\bar{\sigma}_{1i}, \bar{\sigma}_{2i})$ in (13).
Case 1 If $\bar{\sigma}_{1,i}(\cdot) = 0$ for all $i = 1,2,3$, then there exists a finite $T_{01}(\tilde{q}_v(0), \bar{\delta}_1) > 0$ such that $\lim_{t\to T_{01}} \tilde{\omega}(t) = 0$, $\lim_{t\to T_{01}} \tilde{q}_v(t) = 0$, see Lemma 3.3 in [13].
Case 2 If $\bar{\sigma}_{1,i}(\cdot) \neq 0$ and $|\tilde{q}_{v,i}| \leq \phi_q$ for some i, then it follows from $|\sigma_i| \leq \bar{\delta}_0$ and definition of σ_i in (13) that

$$|\tilde{\omega}_i + c_1\tilde{q}_{v,i} + c_2(l_1\tilde{q}_{v,i} + l_2\tilde{q}_{v,i}^{[2]})| \leq \bar{\delta}_0,$$

and consequently, from the definitions of l_1 and l_2 and $|\tilde{q}_{v,i}| \leq \phi_q$,

$$\begin{aligned}|\tilde{\omega}_i| &\leq \bar{\delta}_0 + c_1|\tilde{q}_{v,i}| + c_2|l_1\tilde{q}_{v,i}| + c_2|l_2\tilde{q}_{v,i}^{[2]}| \\ &\leq \bar{\delta}_0 + c_1\phi_q + c_2\phi_q^r.\end{aligned}$$

Case 3 If $\bar{\sigma}_{1,i}(\cdot) \neq 0$ and $|\tilde{q}_{v,i}| > \phi_q$, then $|\tilde{\omega}_i + c_1\tilde{q}_{v,i} + c_2\tilde{q}_{v,i}^{[r]}| \leq \bar{\delta}_0$. Two cases should be discussed.
(i) $\tilde{\omega}_i + c_1\tilde{q}_{v,i} + c_2\tilde{q}_{v,i}^{[r]} \geq 0$.
First, we show that there exists a positive constant $\bar{\delta}_2$ such that $|\tilde{q}_{v,i}| \leq \bar{\delta}_2$ if $\tilde{\omega}_i + c_1\tilde{q}_{v,i} + c_2\tilde{q}_{v,i}^{[r]} = \bar{\delta}_0$. We rewrite this equality in the following two forms:

$$\begin{aligned}\tilde{\omega}_i + (c_1 - \bar{\delta}_0/\tilde{q}_{v,i})\tilde{q}_{v,i} + c_2\tilde{q}_{v,i}^{[r]} = 0,\\ \tilde{\omega}_i + c_1\tilde{q}_{v,i} + (c_2 - \bar{\delta}_0/\tilde{q}_{v,i}^{[r]})\tilde{q}_{v,i}^{[r]} = 0.\end{aligned}$$

For any given positive constants $\bar{c}_1 < c_1$ and $\bar{c}_2 < c_2$, there exist $\bar{\bar{c}}_1 \in [\bar{c}_1, c_1)$ and $\bar{\bar{c}}_2 \in [\bar{c}_2, c_2)$ such that
$\tilde{\omega}_i + \bar{\bar{c}}_1\tilde{q}_{v,i} + c_2\tilde{q}_{v,i}^{[r]} = 0$ if $|\tilde{q}_{v,i}(t)| \geq \frac{\bar{\delta}_0}{c_1 - \bar{c}_1} > 0$,
$\tilde{\omega}_i + c_1\tilde{q}_{v,i} + \bar{\bar{c}}_1\tilde{q}_{v,i}^{[r]} = 0$ if $|\tilde{q}_{v,i}(t)| \geq \sqrt[r]{\frac{\bar{\delta}_0}{c_2 - \bar{c}_2}} > 0$.
From Lemma 3.3 in [13], for any $|\tilde{q}_{v,i}(0)| > 0$, there exists a finite time $T_{02}(\tilde{q}_{vi}(0), \bar{\delta}_1) > 0$ such that

$$|\tilde{q}_{v,i}(t)| \leq \min\left\{\tfrac{\bar{\delta}_0}{c_1 - \bar{c}_1}, \left(\tfrac{\bar{\delta}_0}{c_2 - \bar{c}_2}\right)^{1/r}\right\} =: \bar{\delta}_2$$

for all $t \geq T_{02}(\tilde{q}_{vi}(0), \bar{\delta}_1)$.
Even if $\bar{\delta}_a := |\tilde{\omega}_i + c_1\tilde{q}_{v,i} + c_2(l_1\tilde{q}_{v,i} + l_2\tilde{q}_{v,i}^{[2]})| < \bar{\delta}_0$. One can show that there exists a finite time $T_{0a}(\tilde{q}_{vi}(0), \bar{\delta}_a) > 0$ such that

$$|\tilde{q}_{v,i}(t)| \leq \min\left\{\tfrac{\bar{\delta}_a}{c_1 - \bar{c}_1}, \left(\tfrac{\bar{\delta}_a}{c_2 - \bar{c}_2}\right)^{1/r}\right\} \leq \bar{\delta}_2$$

for all $t \geq T_{02}(\tilde{q}_{vi}(0), \bar{\delta}_1)$.
Next, from the definition of $\sigma_{1,i}$, we get

$$|\tilde{\omega}_i| \leq \bar{\delta}_1/\varrho + \bar{\epsilon} + c_1\bar{\delta}_2 + c_2\bar{\delta}_2^r.$$

(ii) $\tilde{\omega}_i + c_1\tilde{q}_{v,i} + c_2\tilde{q}_{v,i}^{[r]} < 0$.
First, we show that if $-\tilde{\omega}_i - c_1\tilde{q}_{v,i} - c_2\tilde{q}_{v,i}^{[r]} = \bar{\delta}_0$ then there exists a positive constant $\bar{\delta}_2$ such that $|\tilde{q}_{v,i}| \leq \bar{\delta}_2$. We rewrite it in the following two forms:

$$\begin{aligned}\tilde{\omega}_i + (c_1 + \bar{\delta}_0/\tilde{q}_{v,i})\tilde{q}_{v,i} + c_2\tilde{q}_{v,i}^{[r]} = 0,\\ \tilde{\omega}_i + c_1\tilde{q}_{v,i} + (c_2 + \bar{\delta}_0/\tilde{q}_{v,i}^{[r]})\tilde{q}_{v,i}^{[r]} = 0.\end{aligned}$$

For any given positive constants $\bar{c}_1 < c_1$ and $\bar{c}_2 < c_2$, there exist $\bar{\bar{c}}_1 \in [\bar{c}_1, c_1)$ and $\bar{\bar{c}}_2 \in [\bar{c}_2, c_2)$ such that
$\tilde{\omega}_i + \bar{\bar{c}}_1\tilde{q}_{v,i} + c_2\tilde{q}_{v,i}^{[r]} = 0$, if $|\tilde{q}_{v,i}(t)| \geq \frac{\bar{\delta}_0}{c_1 - \bar{c}_1} > 0$,
$\tilde{\omega}_i + c_1\tilde{q}_{v,i} + \bar{\bar{c}}_2\tilde{q}_{v,i}^{[r]} = 0$, if $|\tilde{q}_{v,i}(t)| \geq \sqrt[r]{\frac{\bar{\delta}_0}{c_2 - \bar{c}_2}} > 0$.
which shows the same solution as case **(i)**, thus we omit the same proof procedure.
Combining the result in Cases 1-3, we have
$|\tilde{q}_{v,i}(\cdot)| \leq \max\{\bar{\delta}_2, \phi_q\}$,
$|\tilde{\omega}_i(\cdot)| \leq \bar{\delta}_1/\varrho + \bar{\epsilon} + c_1\max\{\bar{\delta}_2, \phi_q\} + c_2(\max\{\bar{\delta}_2, \phi_q\})^r$.
for all $i = 1,2,3$ and $t \geq T_*(\tilde{q}_v(0), \bar{\delta}_1)$, where $T_*(\tilde{q}_v(0), \bar{\delta}_1) = \max\{T_{01}(\tilde{q}_v(0), \bar{\delta}_1), T_{02}(\tilde{q}_v(0), \bar{\delta}_1)\}$. That completes the proof. ∎

APPENDIX B
PROOF OF THEOREM 1

Proof of Theorem 1: Consider the following Lyapunov candidate:

$$\begin{aligned}V_1(t, S, \hat{\theta}_1) &:= V_S(t,S) + V_\rho(\hat{\theta}_1), \\ V_S(t,S) &:= \tfrac{1}{2\varrho}S^\top J(t)S, \\ V_\rho(\hat{\theta}_1) &:= \tfrac{1}{2\gamma_S e_{\min}}(\theta_1 - e_{\min}\hat{\theta}_1)^2,\end{aligned} \tag{40}$$

where $e_{\min} > 0$ is defined in Assumption 4, and

$$\theta_1 := \sup_{t\geq 0, z\in\Omega_z} \left\| \left[(W^*(t))^\top, \varepsilon_0(t,z) + D(t)\bar{u}(t) + d(t) \right] \right\|, \tag{41}$$

which is upper bounded from Assumptions 1–3, Remark 4 and $\|\varepsilon_0(\cdot,\cdot)\| \leq \varepsilon_N$.
First, by taking the time derivative of V_S along (24) with (25), it follows from (41) and Assumption 4 that

$$\begin{aligned}\dot{V}_S =& S^\top((W^*)^\top\varphi(z) + \varepsilon_0 + D\bar{u} + d) \\ &- \left(K_S + \hat{\theta}_1\frac{\|\Phi\|}{\|S\|}\right)SDED^\top S \\ \leq& -e_{\min}K_S\|S\|^2 + (\theta_1 - e_{\min}\hat{\theta}_1)\|S\|\|\Phi\|.\end{aligned} \tag{42}$$

Next, by taking the time derivative of V_ρ along the solution to (26), it follows that

$$\dot{V}_\rho = -(\theta_1 - e_{\min}\hat{\theta}_1)\|S\|\|\Phi\| + \tfrac{\gamma_\theta}{\gamma_S}(\theta_1 - e_{\min}\hat{\theta}_1)\hat{\theta}_1.$$

Then, by taking the time derivative of V_1 it follows from Lemma 2 that

$$\dot{V}_1 \le -e_{\min}K_S\|S\|^2 + \tfrac{\gamma_\theta}{\gamma_S}(\theta_1 - e_{\min}\hat{\theta}_1)\hat{\theta}_1 \le -e_{\min}K_S\|S\|^2 - \tfrac{\gamma_\theta}{2\gamma_S e_{\min}}(\theta_1 - e_{\min}\hat{\theta}_1)^2 + \omega_0,$$

$$\omega_0 := \frac{\gamma_\theta}{2\gamma_S e_{\min}}\theta_1^2. \tag{43}$$

Denote $\lambda_1 = \min\{2\varrho e_{\min}K_S/J_{\max}, \gamma_\theta\}$ for $J_{\max}$ in Assumption 3. Then, from (40) and (43)

$$\dot{V}_1 \le -\lambda_1 V_1 + \omega_0.$$

By taking the time integration, it follows that

$$V_1(t) \le \omega_0/\lambda_1 + (V_1(0) - \omega_0/\lambda_1)\, e^{-\lambda_1 t}.$$

From the definition of V_1,

$$\|S(t)\| \le (2\varrho/J_{\min})^{\frac{1}{2}} \left(\omega_0/\lambda_1 + (V_1(0) - \omega_0/\lambda_1)e^{-\lambda_1 t}\right)^{\frac{1}{2}}. \tag{44}$$

Define a positive constant

$$\bar{\delta}_1 := (2\varrho/J_{\min})^{\frac{1}{2}}(\omega_0/\lambda_1)^{\frac{1}{2}}, \tag{45}$$

where $\bar{\delta}_1$ can be made arbitrary small by making γ_S or a pair of K_S and γ_θ sufficiently large, see the definitions of ω_0 and λ_1, respectively. Then, for any $V_1(0) \ge 0$, $\lim_{t\to\infty}\|S^*(t)\| = \bar{\delta}_1$. ∎

Appendix C
Proof of Theorem 2

Theorem 2 is based on the following lemma.

Lemma 4. *Suppose that Assumptions 1–4 hold. Then, one can design the parameters of a TPVS and controller dynamics (27)–(29) such that the following holds: for any positive constant $\bar{\delta}_1 > 0$ and $(S^*(0), \hat{\theta}^*(0), \hat{\eta}^*(0)) \in \mathbb{R}^3\times\mathbb{R}\times\mathbb{R}$, there exists a finite $\bar{T}_2 := \bar{T}_2(S^*(0), \hat{\theta}^*(0), \hat{\eta}^*(0), \bar{\delta}_1) > 0$ such that the solution $S(t)$ to the closed loop system consisting of (24) and (27)–(29) satisfies $\|S^*(\cdot)\| \le \bar{\delta}_1$ for all $t \ge \bar{T}_2$.*

Proof: Consider the following Lyapunov function candidate:

$$V_2(t, S, \hat{\theta}, \hat{\eta}) := V_S(t, S) + V_\rho(\hat{\theta}, \hat{\eta}), \tag{46}$$

$$V_S(t, S) := \tfrac{1}{2\varrho}S^\top J(t)S,$$
$$V_\rho(\hat{\theta}, \hat{\eta}) := \tfrac{1}{2\gamma_S e_{\min}}(\theta - e_{\min}\hat{\theta})^2 + \tfrac{\alpha}{2e_{\min}}(\eta - e_{\min}\hat{\eta})^2,$$

where $e_{\min} > 0$ is defined in Assumption 4, and

$$\theta := \sup_{t\ge 0}\|(W^*(t))^\top\|^2, \tag{47}$$

$$\eta := \sup_{t\ge 0, z\in\Omega_z}\|\varepsilon_0(t, z) + D(t)\bar{u}(t) + d(t)\|, \tag{48}$$

which are upper bounded from Assumptions 1 and 2, Remark 4, and $\|\varepsilon_0(\cdot,\cdot)\| \le \varepsilon_N$.

First, by taking the time derivative of V_S along the solution to (24) with (27) gives

$$\dot{V}_S = S^\top((W^*)^\top\varphi(z) + \varepsilon_0 + D\bar{u} + d) - \left(K_\phi\|S\|^2 + K_S + \tfrac{(K_\rho+\hat{\eta})}{\|S\|} + \tfrac{\|\varphi(z)\|^2}{\phi_\theta}\hat{\theta}\right)S^\top DED^\top S$$
$$\le -e_{\min}K_\phi\|S\|^4 - e_{\min}K_S\|S\|^2 - e_{\min}K_\rho\|S\| + (\eta - e_{\min}\hat{\eta})\|S\| + \sqrt{\theta}\|\varphi(z)\|\|S\| - e_{\min}\hat{\theta}\tfrac{\|\varphi(z)\|^2}{\phi_\theta}\|S\|^2.$$

Note that $\sqrt{\theta}\|S\|\|\varphi(z)\| \le \theta\|S\|^2\|\varphi(z)\|^2/\phi^0 + \phi^0$ for any $\phi^0 > 0$, and thus

$$\dot{V}_S \le -e_{\min}K_\phi\|S\|^4 - e_{\min}K_S\|S\|^2 - e_{\min}K_\rho\|S\| + \phi_\theta + \frac{1}{\phi_\theta}(\theta - e_{\min}\hat{\theta})\|\varphi(z)\|^2\|S\|^2 + (\eta - e_{\min}\hat{\eta})\|S\|. \tag{49}$$

Next, by taking the time derivative of V_ρ along the solutions to (28) and (29), it follows that

$$\dot{V}_\rho = -\tfrac{1}{\gamma_S}(\theta - e_{\min}\hat{\theta})\left(\tfrac{1}{\phi_\theta}\gamma_S\|\varphi(z)\|^2\|S\|^2 - \gamma_\theta\hat{\theta}\right) - \alpha(\eta - e_{\min}\hat{\eta})\left(\tfrac{1}{\alpha}\|S\| - \gamma_\eta\hat{\eta}\right).$$

Then, the time derivative of V_2 satisfies

$$\dot{V}_2 \le -e_{\min}K_\phi\|S\|^4 - e_{\min}K_S\|S\|^2 - e_{\min}K_\rho\|S\| + \phi_\theta + \tfrac{\gamma_\theta}{\gamma_S}(\theta - e_{\min}\hat{\theta})\hat{\theta} + \alpha\gamma_\eta(\eta - e_{\min}\hat{\eta})\hat{\eta}$$
$$\le -e_{\min}K_S\|S\|^2 + \phi_\theta - \tfrac{\gamma_\theta}{2\gamma_S e_{\min}}(\theta - e_{\min}\hat{\theta})^2 + \tfrac{\gamma_\theta}{2\gamma_S e_{\min}}\theta^2 - \tfrac{\alpha\gamma_\eta}{2e_{\min}}(\eta - e_{\min}\hat{\eta})^2 + \tfrac{\alpha\gamma_\eta}{2e_{\min}}\eta^2,$$

where Lemma 2 is used. Let $\lambda_2 := \min\{2e_{\min}\frac{\varrho K_S}{J_{\max}}, \gamma_\theta, \gamma_\eta\}$ and $\lambda_3 := \frac{\gamma_\theta}{2\gamma_S e_{\min}}\theta^2 + \frac{\alpha\gamma_\eta}{2e_{\min}}\delta^2 + \phi_\theta$. Then it follows that

$$\dot{V}_2 \le -\lambda_2 V_2 + \lambda_3,$$

which implies that for any $(S^*(0), \hat{\theta}^*(0), \hat{\eta}^*(0)) \in \mathbb{R}^3\times\mathbb{R}\times\mathbb{R}$, there exist positive constants ε_0, ε_1, ε_2 (depending on $(S^*(0), \hat{\theta}^*(0), \hat{\eta}^*(0))$) such that $\|S(\cdot)\| \le \varepsilon_0$, $|\theta - e_{\min}\hat{\theta}(\cdot)| \le \varepsilon_1$, and $|\eta - e_{\min}\hat{\eta}(\cdot)| \le \varepsilon_2$.

To show the finite-time convergence of S, we again consider inequality (49). From the definition of φ, we have $\|\varphi(\cdot)\| \le h$. From this inequality, it follows that

$$\dot{V}_S \le -e_{\min}K_\phi\|S\|^4 - e_{\min}K_S\|S\|^2 - e_{\min}K_\rho\|S\| + \phi_\theta + \tfrac{\varepsilon_1 h^2}{\phi_\theta}\|S\|^2 + \varepsilon_2\|S\|$$
$$\le -e_{\min}K_\phi\|S\|^4 - e_{\min}K_S\|S\|^2 - e_{\min}K_\rho\|S\| + \phi_\theta + \tfrac{\phi_1}{2\phi_\theta}\|S\|^4 + \tfrac{\phi_2}{2}\|S\|^2 + \tfrac{\varepsilon_1^2 h^4}{2\phi_\theta\phi_1} + \tfrac{\varepsilon_2^2}{2\phi_2},$$

where $\phi_1, \phi_2 > 0$, and the inequalities $\varepsilon_1 h^2\|S\|^2 \le \frac{\phi_1}{2}\|S\|^4 + \frac{\varepsilon_1^2 h^4}{2\phi_1}$ and $\varepsilon_2\|S\| \le \frac{\phi_2}{2}\|S\|^2 + \frac{\varepsilon_2^2}{2\phi_2}$ are used. Choose $K_\phi \ge \frac{\phi_1}{2\phi_\theta e_{\min}}$ and $K_S > \frac{\phi_2}{2e_{\min}}$, and denote $K_{S1} := K_S - \frac{\phi_2}{2e_{\min}}$. Then we have

$$\dot{V}_S \le -e_{\min}K_{S1}\|S\|^2 - e_{\min}K_\rho\|S\| + \bar{\phi}_\theta,$$
$$\bar{\phi}_\theta := \phi_\theta + \tfrac{\varepsilon_1^2 h^4}{2\phi_\theta\phi_1} + \tfrac{\varepsilon_2^2}{2\phi_2}.$$

Let $0 < \lambda_4 < \frac{2e_{\min}\varrho K_{S1}}{J_{\max}}$ and $\lambda_5 := e_{\min}K_\rho\sqrt{\frac{2\varrho}{J_{\max}}}$. If

$$\|S\| \ge \bar{\delta}_{1,1} := \sqrt{\tfrac{2\varrho}{J_{\min}}\tfrac{\bar{\phi}_\theta}{2\varrho e_{\min}K_{S1}/J_{\max} - \lambda_4}},$$

then we have

$$V_S \ge \tfrac{\bar{\phi}_\theta}{2e_{\min}\varrho K_{S1}/J_{\max} - \lambda_4},\ \dot{V}_S + \lambda_4 V_S + \lambda_5 V_S^{\frac{1}{2}} \le 0.$$

Also, let $\lambda_6 := \frac{2\varrho e_{\min}K_{S1}}{J_{\max}}$ and $0 < \lambda_7 < e_{\min}K_\rho\sqrt{\frac{2\varrho}{J_{\max}}}$. If

$$\|S\| \ge \bar{\delta}_{1,2} := \sqrt{\tfrac{2\varrho}{J_{\min}}}\tfrac{\bar{\phi}_\theta}{e_{\min}K_\rho\sqrt{2\varrho/J_{\max}} - \lambda_7},$$

then we have

$$V_S^{1/2} \ge \tfrac{\bar{\phi}_\theta}{e_{\min}K_\rho\sqrt{2\varrho/J_{\max}} - \lambda_7},\ \dot{V}_S + \lambda_6 V_S + \lambda_7 V_S^{\frac{1}{2}} \le 0.$$

Define $\bar{\delta}_1 := \min\{\bar{\delta}_{1,1}, \bar{\delta}_{1,2}\}$. Note that this $\bar{\delta}_1$ can be made arbitrary small by making K_S, K_ρ sufficiently large. According to Lemma 3, for any positive constants $\bar{\delta}_1$, ε_1 and ε_2, and any $\|S^*(0)\|$, there exists $\bar{T}_2 := \bar{T}_2(S^*(0), \hat{\theta}^*(0), \hat{\eta}^*(0), \bar{\delta}_1) > 0$ such that $\|S^*(t)\| \le \bar{\delta}_1$ for all $t \ge \bar{T}_2$. ∎

Remark 7. *One notices that the controller in the previous section given by (25) and (26) can achieve a finite time convergence of $S^*(t)$ to a given bounded set. Indeed, for any $\omega_0/\lambda_1 > 0$ in (45) and $V_1(0) \ge 0$, there exists a finite time $\bar{T}_1 := \bar{T}_1(V_1(0), \omega_0/\lambda_1) > 0$ such that*

$$(V_1(0) - \omega_0/\lambda_1)e^{-\lambda_1 t} \le \omega_0/\lambda_1,\ \forall \bar{T}_1 \ge t.$$

From (44), $\|S(t)\| \le 2\delta_1$ for all $\bar{T}_1 \ge t$. As mentioned in the proof of Theorem 1, $\delta_1 > 0$ can be made arbitrary small. Note that the convergence speed is upper bounded on exponential. However, the controller designed in this section guarantees a faster convergence speed because of the finite time stability result of Lemma 3 in Appendix A.

Theorem 2 follows from Lemmas 1 and 4, and thus its proof is omitted.

Appendix D
Proof of Theorem 3

Theorem 3 is based on the following lemmas.

Lemma 5. *Suppose that Assumptions 1–5 hold. Then, one can design a TPVS and controller dynamics (30)–(35) such that the following holds: for any $(S^*(0), \hat{\theta}^*(0), \hat{\eta}^*(0), \hat{\zeta}^*(0)) \in \mathbb{R}^3 \times \mathbb{R} \times \mathbb{R} \times \mathbb{R}$, there exist four positive constants $\bar{\theta}$, $\bar{\eta}$, $\bar{\zeta}$ and M such that $|\hat{\theta}(\cdot)| \le \bar{\theta}$, $|\hat{\eta}(\cdot)| \le \bar{\eta}$, $|\hat{\zeta}(\cdot)| \le \bar{\zeta}$, and $|\bar{u}_{c,i}| \le M$.*

Proof: In a similar manner as the proof of Lemma 4, one can show that there exists a positive constant δ_v such that
$\|S(\cdot)\| \le (2\varrho/J_{\min})^{\frac{1}{2}} \delta_v^{\frac{1}{2}}$, $|\theta - \bar{e}_{\min}\hat{\theta}(\cdot)| \le 2\gamma_S \bar{e}_{\min} \delta_v^{\frac{1}{2}}$,
$|\eta - \bar{e}_{\min}\xi\hat{\eta}(\cdot)| \le \frac{2\bar{e}_{\min}\xi}{\alpha}\delta_v^{\frac{1}{2}}$,
where θ and η are defined by (47) and (48), respectively. From the triangular inequality, we have $|\hat{\theta}(\cdot)| \le \bar{\theta}$ with $\bar{\theta} := 2\gamma_S \delta_v^{\frac{1}{2}} + \frac{\theta}{\bar{e}_{\min}}$ and $|\hat{\eta}(\cdot)| \le \bar{\eta}$ with $\bar{\eta} := \frac{2}{\alpha}\delta_v^{\frac{1}{2}} + \frac{\eta}{\bar{e}_{\min}\xi}$.

Next, we move on to find the upper bound of $\hat{\zeta}$. Based on (35), we consider the following two cases:

Case 1. If $\zeta_\hbar \ge 0$, then $|\hat{\zeta}(\cdot)| \le (K_\rho + \bar{\eta})(2\varrho/J_{\max})^{\frac{1}{2}} \delta_v^{\frac{1}{2}}/\gamma_\zeta$;

Case 2. If $\zeta_\hbar < 0$, then $\dot{\hat{\zeta}} \le 0$, which means that $|\hat{\zeta}(\cdot)| \le \hat{\zeta}(0)$. Then, $|\hat{\zeta}(\cdot)| \le \bar{\zeta}$ for $\bar{\zeta} := \max\left\{(K_\rho + \bar{\eta})(2\varrho/J_{\max})^{\frac{1}{2}} \delta_v^{\frac{1}{2}}/\gamma_\zeta, \hat{\zeta}(0)\right\}$.

From (32), it follows that $\|\bar{u}_c\| \le M$, where $M := \|D\|\left(\frac{2\varrho\delta_v K_\phi}{J_{\min}} + K_S + \frac{\bar{\theta}h^2}{\phi_\theta}\right)\left(\frac{2\varrho\delta_v}{J_{\min}}\right)^{\frac{1}{2}} + \|D\|\xi\bar{\zeta}(K_\rho + \bar{\eta})$. Therefore, we conclude from $|\bar{u}_{c,i}| \le \|\bar{u}_c\|$ that $|\bar{u}_{c,i}| \le M$. ■

Lemma 6. *Suppose that Assumptions 1–5 hold. Then, one can design a TPVS and controller dynamics (30)–(35) such that the following holds: 1) for any positive constant $u_{\max}$, the designed control input satisfies $|u_{c,i}(\cdot)| \le u_{\max}$, $i = 1, \ldots, n$; 2) for any positive constant $\bar{\delta}_1 > 0$ and $(S^*(0), \hat{\theta}^*(0), \hat{\eta}^*(0), \hat{\zeta}^*(0)) \in \mathbb{R}^3 \times \mathbb{R} \times \mathbb{R} \times \mathbb{R}$, there exists a finite $\bar{T}_3 := \bar{T}_3(S^*(0), \hat{\theta}^*(0), \hat{\eta}^*(0), \hat{\zeta}^*(0), \bar{\delta}_1) > 0$ such that the solution $S(t)$ to the closed loop system consisting of (24) and (32)–(35) satisfies $\|S^*(\cdot)\| \le \bar{\delta}_1$ for all $t \ge \bar{T}_3$.*

Proof: Consider the following Lyapunov function candidate:

$$V_3(t, S, \hat{\theta}, \hat{\eta}, \hat{\zeta}) := V_S(t, S) + V_\rho(\hat{\theta}), \tag{50}$$

$$V_S(t, S) := \tfrac{1}{2\varrho} S^\top J(t) S\,,$$

$$V_\rho(\hat{\theta}, \hat{\eta}, \hat{\zeta}) := \frac{1}{2\gamma_S e_{\min}\underline{\zeta}}(\theta - e_{\min}\underline{\zeta}\hat{\theta})^2 + \frac{\alpha}{2e_{\min}\underline{\zeta}\xi}(\eta - e_{\min}\underline{\zeta}\xi\hat{\eta})^2 + \frac{e_{\min}\underline{\zeta}}{2\beta}\left(\hat{\zeta}^{-1} - \bar{\zeta}^{-1}\right)^2,$$

where $e_{\min} > 0$ is defined in Assumption 4, $\xi > 1$ is a design parameter, $\underline{\zeta}$ is given in (37), $\bar{\zeta}$ is the upper bound of $\hat{\zeta}$ in Lemma 5, and θ and η are defined by (47) and (48), respectively.

First, by taking the time derivative of V_S along the solution to (24) with (32) gives

$$\begin{aligned}\dot{V}_S &\le S^\top((W^*)^\top\varphi(z) + \varepsilon_0 + D\bar{u} + d) - \underline{\zeta}\left(K_\phi\|S\|^2 + K_S + \frac{\|\varphi(z)\|^2}{\phi_\theta}\hat{\theta} + \xi\hat{\zeta}\frac{(K_\rho+\hat{\eta})}{\|S\|}\right) S^\top D E D^\top S \\ &\le -e_{\min}\underline{\zeta}K_\phi\|S\|^4 - e_{\min}\underline{\zeta}K_S\|S\|^2 - e_{\min}\underline{\zeta}\xi\hat{\zeta}(K_\rho+\hat{\eta})\|S\| + \eta\|S\| + \sqrt{\theta}\|\varphi(z)\|\|S\| - e_{\min}\underline{\zeta}\hat{\theta}\frac{\|\varphi(z)\|^2}{\phi_\theta}\|S\|^2.\end{aligned}$$

Note that $\sqrt{\theta}\|S\|\|\varphi(z)\| \le \theta\|S\|^2\|\varphi(z)\|^2/\phi^0 + \phi^0$ for any $\phi^0 > 0$, and thus

$$\dot{V}_S \le -e_{\min}\underline{\zeta}K_\phi\|S\|^4 - e_{\min}\underline{\zeta}K_S\|S\|^2 + \eta\|S\| + \phi_\theta - e_{\min}\underline{\zeta}\xi\hat{\zeta}(K_\rho+\hat{\eta})\|S\| + \frac{\|\varphi(z)\|^2}{\phi_\theta}(\theta - e_{\min}\underline{\zeta}\hat{\theta})\|S\|^2. \tag{51}$$

Next, by taking the time derivative of V_ρ along the solutions to (33)-(34), it follows that

$$\begin{aligned}\dot{V}_\rho = &-\frac{\|\varphi(z)\|^2}{\phi_\theta}(\theta - e_{\min}\underline{\zeta}\hat{\theta})\|S\|^2 + \frac{\gamma_\theta}{\gamma_S}(\theta - e_{\min}\underline{\zeta}\hat{\theta})\hat{\theta} \\ &- (\eta - e_{\min}\underline{\zeta}\xi\hat{\eta})\|S\| + \alpha\gamma_\eta(\eta - e_{\min}\underline{\zeta}\xi\hat{\eta})\hat{\eta} \\ &- \frac{e_{\min}\underline{\zeta}}{\beta\hat{\zeta}^2}\left(\hat{\zeta}^{-1} - \bar{\zeta}^{-1}\right)\dot{\hat{\zeta}}.\end{aligned} \tag{52}$$

Then two cases are discussed based on the adaptation law (35).

Case 1 If $\hat{\zeta} > \underline{1}$ or if $\hat{\zeta} = 1$ and $\zeta_\hbar \ge 0$, then

$$\dot{\hat{\zeta}} = \beta\xi\hat{\zeta}^3[(K_\rho + \hat{\eta})\|S\| - \gamma_\zeta\hat{\zeta}].$$

Substituting it into (52) and combining (51) and (52), the time derivative of V_3 satisfies

$$\begin{aligned}\dot{V}_3 \le &-e_{\min}\underline{\zeta}K_\phi\|S\|^4 - e_{\min}\underline{\zeta}K_S\|S\|^2 + \eta\|S\| \\ &-e_{\min}\underline{\zeta}\xi\hat{\zeta}(K_\rho+\hat{\eta})\|S\| + \tfrac{\gamma_\theta}{\gamma_S}(\theta - e_{\min}\underline{\zeta}\hat{\theta})\hat{\theta} \\ &-(\eta - e_{\min}\underline{\zeta}\xi\hat{\eta})\|S\| + \alpha\gamma_\eta(\eta - e_{\min}\underline{\zeta}\xi\hat{\eta})\hat{\eta} + \phi_\theta \\ &-e_{\min}\underline{\zeta}\xi\hat{\zeta}\left(\hat{\zeta}^{-1} - \bar{\zeta}^{-1}\right)\left[(K_\rho+\hat{\eta})\|S\| - \gamma_\zeta\hat{\zeta}\right],\end{aligned} \tag{53}$$

and consequently, from the definition of $\bar{\zeta}$ in Lemma 5 in Appendix, $(\bar{\zeta}^{-1} - 1) \le 0$. Thus we derive

$$\begin{aligned}&-e_{\min}\underline{\zeta}\xi\hat{\zeta}(K_\rho+\hat{\eta})\|S\| - e_{\min}\underline{\zeta}\xi\hat{\zeta}(\hat{\zeta}^{-1} - \bar{\zeta}^{-1})(K_\rho+\hat{\eta})\|S\| \\ &= (\bar{\zeta}^{-1} - 1)e_{\min}\underline{\zeta}\xi\hat{\zeta}(K_\rho+\hat{\eta})\|S\| - e_{\min}\underline{\zeta}\xi(K_\rho+\hat{\eta})\|S\| \\ &\le -e_{\min}\underline{\zeta}\xi(K_\rho+\hat{\eta})\|S\|.\end{aligned} \tag{54}$$

By combining $\eta\|S\|$ in (53) and $-e_{\min}\underline{\zeta}\xi\hat{\eta}\|S\|$ in (54), the time derivative of V_3 becomes

$$\begin{aligned}\dot{V}_3 \le &-e_{\min}\underline{\zeta}K_\phi\|S\|^4 - e_{\min}\underline{\zeta}K_S\|S\|^2 - e_{\min}\underline{\zeta}\xi K_\rho\|S\| \\ &+\tfrac{\gamma_\theta}{\gamma_S}(\theta - e_{\min}\underline{\zeta}\hat{\theta})\hat{\theta} + \alpha\gamma_\eta(\eta - e_{\min}\underline{\zeta}\xi\hat{\eta})\hat{\eta} \\ &+e_{\min}\underline{\zeta}\xi\hat{\zeta}\left(\hat{\zeta}^{-1} - \bar{\zeta}^{-1}\right)\gamma_\zeta\hat{\zeta} + \phi_\theta,\end{aligned} \tag{55}$$

where the term $(\eta - e_{\min}\underline{\zeta}\xi\hat{\eta})\|S\|$ is counteracted. From Lemma 2, the following inequalities hold.

$$\frac{\gamma_\theta}{\gamma_S}(\theta - e_{\min}\underline{\zeta}\hat{\theta})\hat{\theta} \le -\frac{\gamma_\theta(\theta - e_{\min}\underline{\zeta}\hat{\theta})^2}{2\gamma_S e_{\min}\underline{\zeta}} + \frac{\gamma_\theta\theta^2}{2\gamma_S e_{\min}\underline{\zeta}}, \tag{56}$$

$$\alpha\gamma_\eta(\eta - e_{\min}\underline{\zeta}\xi\hat{\eta})\hat{\eta} \le -\frac{\alpha\gamma_\eta(\eta - e_{\min}\underline{\zeta}\xi\hat{\eta})^2}{2e_{\min}\underline{\zeta}\xi} + \frac{\alpha\gamma_\eta\eta^2}{2e_{\min}\underline{\zeta}\xi}.$$

Furthermore, the following equation is true

$$e_{\min}\underline{\zeta}\xi\hat{\zeta}(\hat{\zeta}^{-1} - \bar{\zeta}^{-1})\gamma_\zeta\hat{\zeta} = -e_{\min}\underline{\zeta}\xi\gamma_\zeta\bar{\zeta}^{-1}[(\hat{\zeta} - \tfrac{\bar{\zeta}}{2})^2 - \tfrac{\bar{\zeta}^2}{4}]. \tag{57}$$

Note that $-e_{\min}\underline{\zeta}\xi\gamma_\zeta\bar{\zeta}^{-1}(\hat{\zeta}-\frac{\bar{\zeta}}{2})^2\leq 0$. Then by adding and subtracting $e_{\min}\underline{\zeta}\xi\gamma_\zeta(\hat{\zeta}^{-1}-\bar{\zeta}^{-1})^2$, and substituting (56)–(57) into (55), it follows that

$$\dot{V}_3\leq -e_{\min}\underline{\zeta}K_S\|S\|^2-\frac{\gamma_\theta}{2\gamma_S e_{\min}\underline{\zeta}}(\theta-e_{\min}\underline{\zeta}\hat{\theta})^2+\phi_\theta$$
$$-\frac{\alpha\gamma_\eta}{2e_{\min}\underline{\zeta}\xi}(\eta-e_{\min}\underline{\zeta}\xi\hat{\eta})^2+\frac{\alpha\gamma_\eta}{2e_{\min}\underline{\zeta}\xi}\eta^2+\frac{\gamma_\theta}{2\gamma_S e_{\min}\underline{\zeta}}\theta^2$$
$$+e_{\min}\underline{\zeta}\xi\gamma_\zeta\left[(\hat{\zeta}^{-1}-\bar{\zeta}^{-1})^2+\frac{\bar{\zeta}}{4}\right]-e_{\min}\underline{\zeta}\xi\gamma_\zeta(\hat{\zeta}^{-1}-\bar{\zeta}^{-1})^2.$$

Invoking the fact $\hat{\zeta}^{-1}\geq\bar{\zeta}^{-1}>0$ and $\hat{\zeta}^{-1}\in(0,1]$, it has

$$e_{\min}\underline{\zeta}\xi\gamma_\zeta\left[(\hat{\zeta}^{-1}-\bar{\zeta}^{-1})^2+\bar{\zeta}/4\right]\leq e_{\min}\underline{\zeta}\xi\gamma_\zeta(1+\bar{\zeta}/4).$$

Let $\lambda_8=\min\{\frac{2\varrho e_{\min}\underline{\zeta}K_S}{J_{\max}},\gamma_\theta,\gamma_\eta,2\xi\gamma_\zeta\beta\}$, $\lambda_9=\frac{\gamma_\theta}{2\gamma_S e_{\min}\underline{\zeta}}\theta^2+\frac{\alpha\gamma_\eta}{2e_{\min}\underline{\zeta}\xi}\eta^2+e_{\min}\underline{\zeta}\xi\gamma_\zeta(1+\bar{\zeta}/4)+\phi_\theta$. Then it follows that

$$\dot{V}_3\leq-\lambda_8V_2+\lambda_9,$$

which implies that for any $(S^*(0),\hat{\theta}^*(0),\hat{\eta}^*(0),\hat{\zeta}^*(0))\in\mathbb{R}^3\times\mathbb{R}\times\mathbb{R}\times\mathbb{R}$, there exist positive constants ε_3, ε_4, ε_5, ε_6 (depending on $(S^*(0),\hat{\theta}^*(0),\hat{\eta}^*(0),\hat{\zeta}^*(0))$) such that $\|S(\cdot)\|\leq\varepsilon_3$, $|\theta-e_{\min}\underline{\zeta}\hat{\theta}(\cdot)|\leq\varepsilon_4$, $|\eta-e_{\min}\underline{\zeta}\xi\hat{\eta}(\cdot)|\leq\varepsilon_5$, and $|\hat{\zeta}^{-1}(\cdot)-\bar{\zeta}^{-1}|\leq\varepsilon_6$.

To show the finite-time convergence of S, we again consider inequality (51). According to $\hat{\zeta}\geq 1$ in (35) and $\|\varphi(\cdot)\|\leq h$ and $\bar{\eta}\geq\hat{\eta}$ from Lemma 5, it follows that

$$\dot{V}_S\leq-e_{\min}\underline{\zeta}K_\phi\|S\|^4-e_{\min}\underline{\zeta}K_S\|S\|^2-e_{\min}\underline{\zeta}\xi K_\rho\|S\|$$
$$+\tfrac{1}{2\phi_\theta\phi_3}(\theta-e_{\min}\underline{\zeta}\hat{\theta})^2\|\varphi(z)\|^4+\tfrac{\phi_3}{2\phi_\theta}\|S\|^4$$
$$+\tfrac{1}{2\phi_4}(\eta-e_{\min}\underline{\zeta}\xi\hat{\eta})^2+\tfrac{\phi_4}{2}\|S\|^2+\tfrac{\phi_5}{2}\|S\|^2+\phi_\theta,$$

where ϕ_3, $\phi_4>0$, and the following inequalities are used.

$$\tfrac{\|\varphi(z)\|^2}{\phi_\theta}(\theta-e_{\min}\underline{\zeta}\hat{\theta})\|S\|^2\leq$$
$$\tfrac{1}{2\phi_\theta\phi_3}(\theta-e_{\min}\underline{\zeta}\hat{\theta})^2\|\varphi(z)\|^4+\tfrac{\phi_3}{2\phi_\theta}\|S\|^4,$$
$$(\eta-e_{\min}\underline{\zeta}\xi\hat{\eta})\|S\|\leq\tfrac{1}{2\phi_4}(\eta-e_{\min}\underline{\zeta}\xi\hat{\eta})^2+\tfrac{\phi_4}{2}\|S\|^2,$$
$$-e_{\min}\underline{\zeta}\xi\hat{\zeta}K_\rho\|S\|\leq-e_{\min}\underline{\zeta}\xi K_\rho\|S\|,$$
$$-e_{\min}\underline{\zeta}\xi\hat{\zeta}\hat{\eta}\|S\|\leq-e_{\min}\underline{\zeta}\xi\hat{\eta}\|S\|.$$

Choose $K_\phi\geq\frac{\phi_3}{2\phi_\theta\underline{\zeta}e_{\min}}$, $K_S>\frac{\phi_4}{2\underline{\zeta}e_{\min}}$, and denote $K_{S2}>K_S-\frac{\phi_4}{2\underline{\zeta}e_{\min}}$. Then we have

$$\dot{V}_S\leq-e_{\min}\underline{\zeta}K_{S2}\|S\|^2-e_{\min}\underline{\zeta}\xi K_\rho\|S\|+\bar{\phi}^1,$$
$$\bar{\phi}^1:=\phi_\theta+\tfrac{\varepsilon_4^2h^4}{2\phi_\theta\phi_3}+\tfrac{\varepsilon_5^2}{2\phi_4}.$$

Let $0<\lambda_8<\frac{2\varrho e_{\min}\underline{\zeta}K_{S2}}{J_{\max}}$ and $\lambda_9:=e_{\min}\underline{\zeta}\xi K_\rho\sqrt{\frac{2\varrho}{J_{\max}}}$. If

$$\|S\|\geq\bar{\delta}_{1,3}:=\sqrt{\tfrac{2\varrho}{J_{\min}}}\tfrac{\bar{\phi}^1}{2\varrho e_{\min}\underline{\zeta}K_{S2}/J_{\max}-\lambda_8},$$

then we have

$$V_S\geq\tfrac{\bar{\phi}^1}{2\varrho e_{\min}\underline{\zeta}K_{S2}/J_{\max}-\lambda_8},\ \dot{V}_S+\lambda_8V_S+\lambda_9V_S^{\frac{1}{2}}\leq 0.$$

Also, let $\lambda_{10}:=\frac{2\varrho e_{\min}\underline{\zeta}K_{S2}}{J_{\max}}$ and $0<\lambda_{11}<e_{\min}\underline{\zeta}\xi K_\rho\sqrt{\frac{2\varrho}{J_{\max}}}$. If $\|S\|\geq\bar{\delta}_{1,4}:=\sqrt{\frac{2\varrho}{J_{\min}}}\frac{\bar{\phi}^1}{e_{\min}\underline{\zeta}\xi K_\rho\sqrt{2\varrho/J_{\max}}-\lambda_{11}}$, then we have

$$V_S^{1/2}\geq\tfrac{\bar{\phi}_\theta}{e_{\min}\underline{\zeta}\xi K_\rho\sqrt{2\varrho/J_{\max}}-\lambda_{11}},\ \dot{V}_S+\lambda_{10}V_S+\lambda_{11}V_S^{\frac{1}{2}}\leq 0.$$

Denote $\bar{\delta}_{c1}:=\min\{\bar{\delta}_{1,3},\bar{\delta}_{1,4}\}$. Note that this $\bar{\delta}_{c1}$ can be made arbitrary small by making K_S, K_ρ sufficiently large. According to Lemma 3, for any positive constants $\bar{\delta}_{c1}$, ε_4, and ε_5, and any $(S^*(0),\hat{\theta}^*(0),\hat{\eta}^*(0),\hat{\zeta}^*(0))\in\mathbb{R}^3\times\mathbb{R}\times\mathbb{R}\times\mathbb{R}$, there exist a $\bar{T}_{c1}:=\bar{T}_{c1}(S^*(0),\hat{\theta}^*(0),\hat{\eta}^*(0),\hat{\zeta}^*(0),\bar{\delta}_{c1})>0$ such that $\|S^*(t)\|\leq\bar{\delta}_{c1}$ for all $t\geq\bar{T}_{c1}$.

Case 2 If $\hat{\zeta}=1$ and $\zeta_\hbar<0$, then $\dot{\hat{\zeta}}=0$ can be obtained from the adaptation law Eq. (35). In this situation, the input saturation does not exist and $\hat{\zeta}=1$. Substituting $\hat{\zeta}=1$ into (32), it has

$$u_c=-D^\top(K_\phi\|S\|^2+K_S+\tfrac{1}{\phi_0}\hat{\theta}\|\varphi(z)\|^2)S-D^\top\xi\tfrac{(K_\rho+\hat{\eta})S}{\|S\|},$$

which is similar to the control law (27) except for the constant gain ξ. Following the proof of *Lemma 4*, one can also proof that for any positive constant $\bar{\delta}_{c2}>0$ and $(S^*(0),\hat{\theta}^*(0),\hat{\eta}^*(0))\in\mathbb{R}^3\times\mathbb{R}\times\mathbb{R}$, there exists a $\bar{T}_{c2}:=\bar{T}_{c2}(S^*(0),\hat{\theta}^*(0),\hat{\eta}^*(0),\bar{\delta}_{c2})>0$ such that $\|S^*(\cdot)\|\leq\bar{\delta}_{c2}$ for all $t\geq\bar{T}_{c2}$, where $\bar{\delta}_{c2}:=\max\{\bar{\delta}_{1,5},\bar{\delta}_{1,6}\}$, $\bar{\delta}_{1,5}:=\sqrt{\frac{2\varrho}{J_{\min}}}\frac{\bar{\phi}^2}{2\varrho e_{\min}K_{S1}/J_{\max}-\lambda_4}$, $\bar{\delta}_{1,6}:=\sqrt{\frac{2\varrho}{J_{\min}}}\frac{\bar{\phi}^2}{e_{\min}\xi K_\rho\sqrt{2\varrho/J_{\max}}-\lambda_{12}}$, $\bar{\phi}^2:=\phi_\theta+\frac{\varepsilon_1^2h^4}{2\phi_\theta\phi_1}+\frac{\varepsilon_7^2}{2\phi_2}$, $\lambda_{12}:=e_{\min}\xi K_\rho\sqrt{\frac{2\varrho}{J_{\max}}}$, $\varepsilon_7>0$ satisfied $|\eta-e_{\min}\xi\hat{\eta}(\cdot)|\leq\varepsilon_7$.

Define $\bar{\delta}_1:=\{\bar{\delta}_{c1},\bar{\delta}_{c2}\}$, $\bar{T}_3:=\max\{\bar{T}_{c1}(S^*(0),\hat{\theta}^*(0),\hat{\eta}^*(0),\hat{\zeta}^*(0),\bar{\delta}_{c1}),\bar{T}_{c2}(S^*(0),\hat{\theta}^*(0),\hat{\eta}^*(0),\bar{\delta}_{c2})\}$ which is related to the initial values $S^*(0),\hat{\theta}^*(0),\hat{\eta}^*(0),\hat{\zeta}^*(0)$ and $\bar{\delta}_1$.

Finally, summarizing Cases 1 and 2, it can be concluded that for any positive constant $\bar{\delta}_1>0$ and $(S^*(0),\hat{\theta}^*(0),\hat{\eta}^*(0),\hat{\zeta}^*(0))\in\mathbb{R}^3\times\mathbb{R}\times\mathbb{R}\times\mathbb{R}$, there exists a finite $\bar{T}_3:=\bar{T}_3(S^*(0),\hat{\theta}^*(0),\hat{\eta}^*(0),\hat{\zeta}^*(0),\bar{\delta}_1)>0$ such that the solution $S(t)$ to the closed loop system consisting of (24) and (32)–(35) satisfies $\|S^*(\cdot)\|\leq\bar{\delta}_1$ for all $t\geq\bar{T}_3$.
That completes the proof. ■

The proof of Theorem 3 follows from Lemmas 1 and 6, and thus is omitted.

REFERENCES

[1] W. Cai, X. Liao, and D. Y. Song, "Indirect robust adaptive fault-tolerant control for attitude tracking of spacecraft," *Journal of Guidance, Control, and Dynamics*, vol. 31, no. 5, pp. 1456–1463, 2008.

[2] A. Benallegue, Y. Chitour, and A. Tayebi, "Adaptive attitude tracking control of rigid body systems with unknown inertia and gyro-bias," *IEEE Transactions on Automatic Control*, vol. 63, no. 11, pp. 3986–3993, 2018.

[3] Y. Wang, H. R. Karimi, H. Shen, Z. Fang, and M. Liu, "Fuzzy-model-based sliding mode control of nonlinear descriptor systems," *IEEE Transactions on Cybernetics*, no. 99, pp. 1–11, 2018.

[4] Q. Hu and B. Jiang, "Continuous finite-time attitude control for rigid spacecraft based on angular velocity observer," *IEEE Transactions on Aerospace and Electronic Systems*, vol. 54, no. 3, pp. 1082–1092, 2018.

[5] Y. Wang, H. Shen, H. R. Karimi, and D. Duan, "Dissipativity-based fuzzy integral sliding mode control of continuous-time ts fuzzy systems," *IEEE Transactions on Fuzzy Systems*, vol. 26, no. 3, pp. 1164–1176, 2018.

[6] X. Cao, P. Shi, Z. Li, and M. Liu, "Neural-network-based adaptive backstepping control with application to spacecraft attitude regulation," *IEEE Transactions on Neural Networks and Learning Systems*, vol. 29, no. 9, pp. 4303–4313, 2018.

[7] Y. Wang, X. Yang, and H. Yan, "Reliable fuzzy tracking control of near-space hypersonic vehicle using aperiodic measurement information," *IEEE Transactions on Industrial Electronics*, 2019.

[8] L. Sun and Z. Zheng, "Saturated adaptive hierarchical fuzzy attitude-tracking control of rigid spacecraft with modeling and measurement uncertainties," *IEEE Transactions on Industrial Electronics*, vol. 66, no. 5, pp. 3742–3751, 2019.

[9] S. Berkane, A. Abdessameud, and A. Tayebi, "Hybrid output feedback for attitude tracking on SO(3)," *IEEE Transactions on Automatic Control*, vol. 63, no. 11, pp. 3956–3963, 2018.

[10] Y. Xia, Z. Zhu, M. Fu, and S. Wang, "Attitude tracking of rigid spacecraft with bounded disturbances," *IEEE Transactions on Industrial Electronics*, vol. 58, no. 2, pp. 647–659, 2011.

[11] C. Zhang, J. Wang, D. Zhang, and X. Shao, "Learning observer based and event-triggered control to spacecraft against actuator faults," *Aerospace Science and Technology*, vol. 78, pp. 522–530, 2018.

[12] F. Bayat, "Model predictive sliding control for finite-time three-axis spacecraft attitude tracking," *IEEE Transactions on Industrial Electronics*, 2018.

[13] K. Lu and Y. Xia, "Adaptive attitude tracking control for rigid spacecraft with finite-time convergence," *Automatica*, vol. 49, no. 12, pp. 3591–3599, 2013.

[14] Q. Chen, S. Xie, M. Sun, and X. He, "Adaptive non-singular fixed-time attitude stabilization of uncertain spacecraft," *IEEE Transactions on Aerospace and Electronic Systems*, 2018.

[15] K. Lu, Y. Xia, C. Yu, and H. Liu, "Finite-time tracking control of rigid spacecraft under actuator saturations and faults," *IEEE Transactions on Automation Science and Engineering*, vol. 1, no. 13, pp. 368–381, 2016.

[16] N. Zhou and Y. Xia, "Distributed fault-tolerant control design for spacecraft finite-time attitude synchronization," *International Journal of Robust and Nonlinear Control*, vol. 26, no. 14, pp. 2994–3017, 2016.

[17] M. Blanke, R. Izadi-Zamanabadi, S. A. Bøgh, and C. P. Lunau, "Fault-tolerant control systemsa holistic view," *Control Engineering Practice*, vol. 5, no. 5, pp. 693–702, 1997.

[18] T. Chen and H. Chen, "Approximation capability to functions of several variables, nonlinear functionals, and operators by radial basis function neural networks," *IEEE Transactions on Neural Networks*, vol. 6, no. 4, pp. 904–910, 1995.

[19] Y. Zou and Z. Zheng, "A robust adaptive RBFNN augmenting backstepping control approach for a model-scaled helicopter," *IEEE Transactions on Control Systems Technology*, vol. 23, no. 6, pp. 2344–2352, 2015.

[20] G. Wen, S. S. Ge, F. Tu, and Y. S. Choo, "Artificial potential-based adaptive h_∞ synchronized tracking control for accommodation vessel," *IEEE Transactions on Industrial Electronics*, vol. 64, no. 7, pp. 5640–5647, 2017.

[21] Q. Shen, D. Wang, S. Zhu, and K. Poh, "Finite-time fault-tolerant attitude stabilization for spacecraft with actuator saturation," *IEEE Transactions on Aerospace and Electronic Systems*, vol. 51, no. 3, pp. 2390–2405, 2015.

[22] B. Jiang, Q. Hu, and M. I. Friswell, "Fixed-time attitude control for rigid spacecraft with actuator saturation and faults," *IEEE Transactions on Control Systems Technology*, vol. 24, no. 5, pp. 1892–1898, 2016.

[23] B. Li, Q. Hu, Y. Yu, and G. Ma, "Observer-based fault-tolerant attitude control for rigid spacecraft," *IEEE Transactions on Aerospace and Electronic Systems*, vol. 53, no. 5, pp. 2572–2582, 2017.

[24] H. Dong, Q. Hu, M. I. Friswell, and G. Ma, "Dual-quaternion-based fault-tolerant control for spacecraft tracking with finite-time convergence," *IEEE Transactions on Control Systems Technology*, vol. 25, no. 4, pp. 1231–1242, 2017.

[25] B. Xiao, Q. Hu, D. Wang, and E. K. Poh, "Attitude tracking control of rigid spacecraft with actuator misalignment and fault," *IEEE Transactions on Control Systems Technology*, vol. 21, no. 6, pp. 2360–2366, 2013.

[26] Q. Hu, X. Shao, and W.-H. Chen, "Robust fault-tolerant tracking control for spacecraft proximity operations using time-varying sliding mode," *IEEE Transactions on Aerospace and Electronic Systems*, vol. 54, no. 1, pp. 2–17, 2018.

[27] B. Huo, Y. Xia, L. Yin, and M. Fu, "Fuzzy adaptive fault-tolerant output feedback attitude-tracking control of rigid spacecraft," *IEEE Transactions on Systems, Man, and Cybernetics: Systems*, vol. 47, no. 8, pp. 1898–1908, 2017.

[28] N. Zhou, Y. Kawano, and M. Cao, "Adaptive failure-tolerant control for spacecraft attitude tracking," *Proceedings of the 15th IFAC Symposium on Large Scale Complex Systems: Theory and Applications, Delft, The Netherlands*, pp. 67–72, May 26-28, 2019.

[29] J. Sidi, Marcel, *Spacecraft Dynamics and Control*. Cambridge University Press, 1997.

[30] M. Blanke, M. Kinnaert, J. Lunze, M. Staroswiecki, and J. Schröder, *Diagnosis and fault-tolerant control*. Springer, 2006, vol. 2.

[31] P. C. Hughes, *Spacecraft Attitude Dynamics*. John Wiley and Sons, New York, 1986.

[32] B. Wu, D. Wang, and E. K. Poh, "Decentralized robust adaptive control for attitude synchronization under directed communication topology," *Journal of Guidance, Control, and Dynamics*, vol. 34, no. 4, pp. 1276–1282, 2011.

[33] L. Wang, T. Chai, and L. Zhai, "Neural-network-based terminal sliding-mode control of robotic manipulators including actuator dynamics," *IEEE Transactions on Industrial Electronics*, vol. 56, no. 9, pp. 3296–3304, 2009.

[34] X. Yu and O. Kaynak, "Sliding-mode control with soft computing: A survey," *IEEE Transactions on Industrial Electronics*, vol. 56, no. 9, pp. 3275–3285, 2009.

[35] L. Cao, D. Qiao, and X. Chen, "Laplace 1 huber based cubature kalman filter for attitude estimation of small satellite," *Acta Astronautica*, vol. 148, pp. 48–56, 2018.

[36] B. Xiao, X. Yang, H. R. Karimi, and J. Qiu, "Asymptotic tracking control for a more representative class of uncertain nonlinear systems with mismatched uncertainties," *IEEE Transactions on Industrial Electronics*, 2019.

[37] B. Xiao and S. Yin, "Exponential tracking control of robotic manipulators with uncertain dynamics and kinematics," *IEEE Transactions on Industrial Informatics*, vol. 15, no. 2, pp. 689–698, 2019.

[38] S. Yu, X. Yu, B. Shirinzadeh, and Z. Man, "Continuous finite-time control for robotic manipulators with terminal sliding mode," *Automatica*, vol. 41, no. 11, pp. 1957–1964, 2005.

Ning Zhou (M'15) received the M.S. degree in applied mathematics from Liaoning University of Technology, Jinzhou, China, in 2011, and the Ph.D. degree in control science and engineering from Beijing Institute of Technology, Beijing, China, in 2015. She was a Postdoctoral Scholar with the Faculty of Science and Engineering, University of Groningen, Groningen, the Netherlands, from Dec. 2017 to Jun. 2019. She is currently a Lecturer with the College of Computer and Information Sciences, Fujian Agriculture and Forestry University, Fuzhou, China. Her research interests include spacecraft attitude synchronization, sliding mode control, fault-tolerant control, and intelligent control.

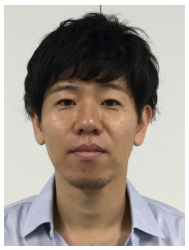

Yu Kawano (M'13) is currently Associate Professor in Department of Mechanical Systems Engineering at Hiroshima University. He received the M.S. and Ph.D. degrees in engineering from Osaka University, Japan, in 2011 and 2013, respectively. From October 2013 to November 2016, he was a Post-Doctoral researcher at both Kyoto University and JST CREST, Japan. From November 2016 to March 2019, he was a Post-Doctoral researcher at the University of Groningen, The Netherlands. He has held visiting research positions at Tallinn University of Technology, Estonia and the University of Groningen and served as a Research Fellow of the Japan Society for the Promotion Science. He is an Associate Editor for *Systems & Control Letters*. His research interests include nonlinear systems, complex networks, and model reduction.

Ming Cao (S'05–M'07–SM'15) received the bachelor's and master's degrees from Tsinghua University, Beijing, China, in 1999 and 2002, respectively, and the Ph.D. degree from Yale University, New Haven, CT, USA, in 2007, all in electrical engineering. He is currently a Professor of Systems and Control with the Engineering and Technology Institute, University of Groningen, Groningen, The Netherlands. Dr. Cao is the 2017 and inaugural recipient of the Manfred Thoma Medal from the International Federation of Automatic Control and the 2016 recipient of the European Control Award sponsored by the European Control Association. He is a Senior Editor for *Systems & Control Letters*, and an Associate Editor for the *IEEE Transactions on Automatic Control* and *IEEE Transactions on Circuits and Systems*.